How is Dark Matter distributed in our local neighborhood?

Nassim Bozorgnia

GRAPPA Center of Excellence
University of Amsterdam

GRAPPA GRavitation AstroParticle Physics Amsterdam

University of Amsterdam

Dark Matter halo

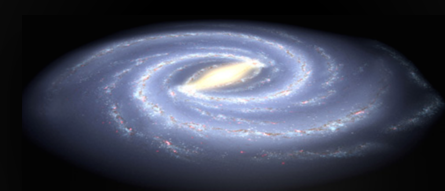

Local Dark Matter distribution

What is the distribution of Dark Matter (DM) in the Sun's neighborhood?

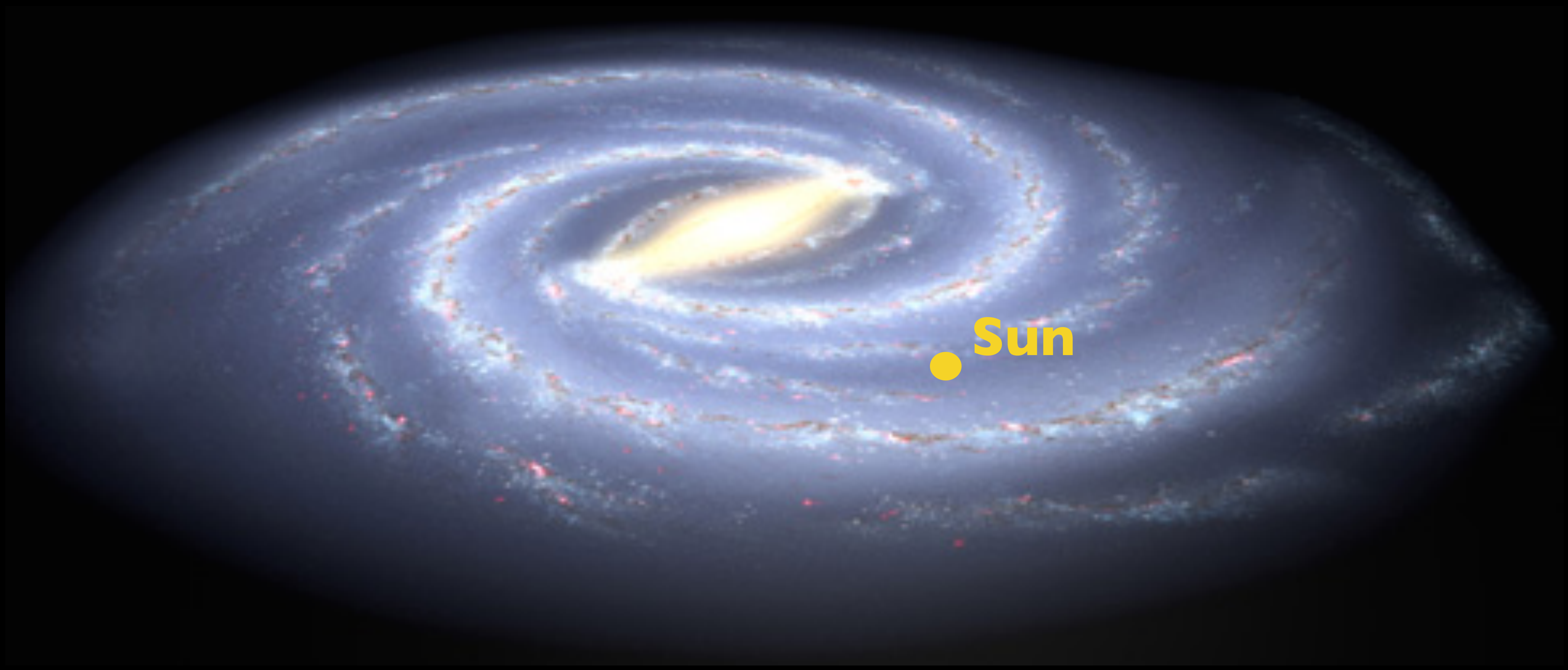

Local Dark Matter distribution

What is the distribution of Dark Matter (DM) in the Sun's neighborhood?

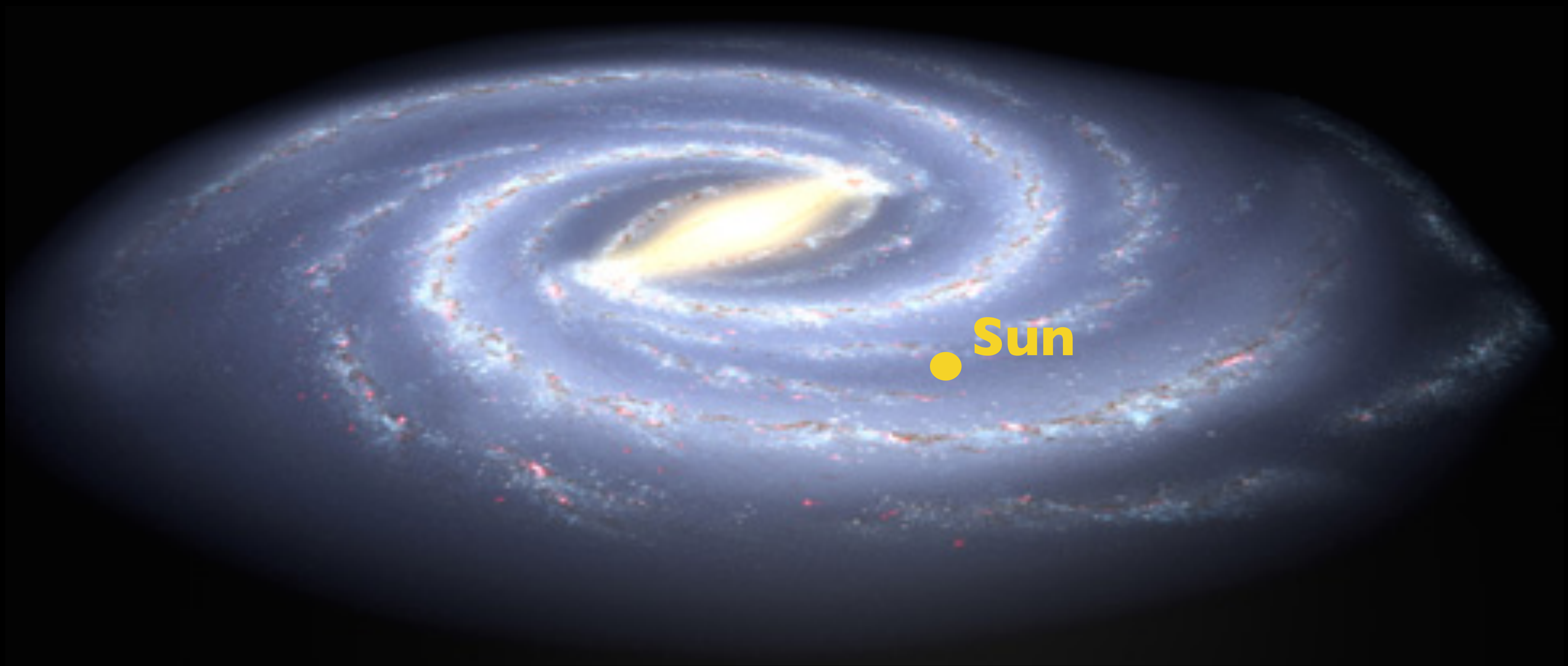

Uncertainties in the local DM distribution → ***prevents a precise determination of the properties of the DM particle when interpreting direct detection data.***

Direct DM detection event rate

- The differential event rate:

$$\frac{dR}{dE_R} = \frac{\rho_\chi}{m_\chi m_N} \int_{v>v_{\min}} d^3v \, \frac{d\sigma_{\chi N}}{dE_R} \, v \, f_{\rm det}(\mathbf{v}, t)$$

where $v_{\min} = \sqrt{m_N E_R/(2\mu_{\chi N}^2)}$ is the minimum DM speed required to produce a recoil energy E_R .

Direct DM detection event rate

- The differential event rate:

astrophysics

$$\frac{dR}{dE_R} = \frac{\rho_\chi}{m_\chi m_N} \int_{v>v_{\rm min}} d^3v \, \frac{d\sigma_{\chi N}}{dE_R} \, v \, f_{\rm det}(\mathbf{v}, t)$$

where $v_{\rm min} = \sqrt{m_N E_R/(2\mu_{\chi N}^2)}$ is the minimum DM speed required to produce a recoil energy E_R .

- **Astrophysical inputs:**
  - **local DM density:** *normalization in event rate.*
  - **local DM velocity distribution:** *enters the event rate through an integration.*

Direct DM detection event rate

- The differential event rate:

$$\frac{dR}{dE_R} = \frac{\rho_\chi}{m_\chi m_N} \int_{v>v_{\min}} d^3v \, \frac{d\sigma_{\chi N}}{dE_R} \, v \, f_{\text{det}}(\mathbf{v}, t)$$

astrophysics (ρ_χ, $f_{\text{det}}(\mathbf{v}, t)$)

- For standard spin-independent and spin-dependent interactions:

$$\frac{dR}{dE_R} = \frac{\sigma_0 F^2(E_R)}{2 m_\chi \mu_{\chi N}^2} \rho_\chi \eta(v_{\min}, t)$$

particle physics: $\frac{\sigma_0 F^2(E_R)}{2 m_\chi \mu_{\chi N}^2}$; astrophysics: $\rho_\chi \eta(v_{\min}, t)$

where

$$\boxed{\eta(v_{\min}, t) \equiv \int_{v>v_{\min}} d^3v \, \frac{f_{\text{det}}(\mathbf{v}, \mathbf{t})}{v}}$$

halo integral

Standard Halo Model

- The simplest model for the DM distribution in our Galaxy is the ***Standard Halo model (SHM)***: isothermal sphere with an isotropic Maxwell-Boltzmann velocity distribution.

Drukier, Freese, Spergel, 1986

Standard Halo Model

- The simplest model for the DM distribution in our Galaxy is the ***Standard Halo model (SHM)***: isothermal sphere with an isotropic Maxwell-Boltzmann velocity distribution.

Drukier, Freese, Spergel, 1986

  - Hydrostatic equilibrium: pressure balances gravitational potential
  - Density profile: $\rho(r) \propto r^{-2}$
  - Local DM density: 0.3 GeV/cm^3
  - Typical DM speed: 220 km/s

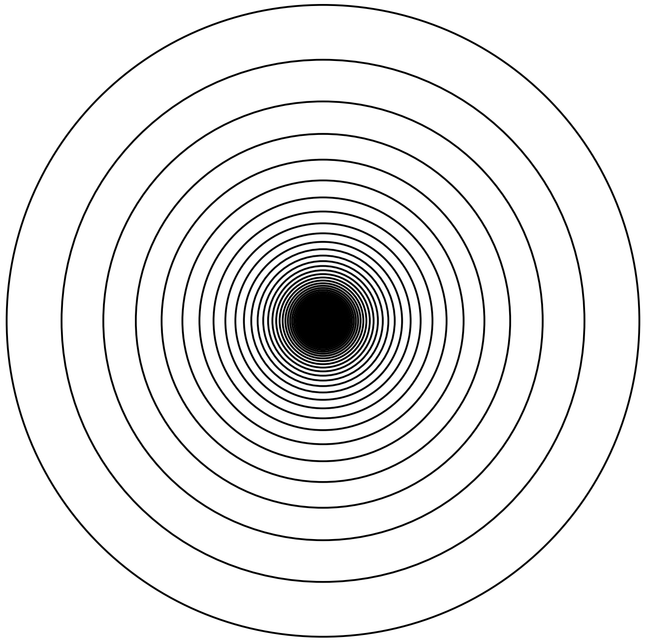

- Actual DM distribution may ***deviate substantially*** from the SHM.

Direct detection results

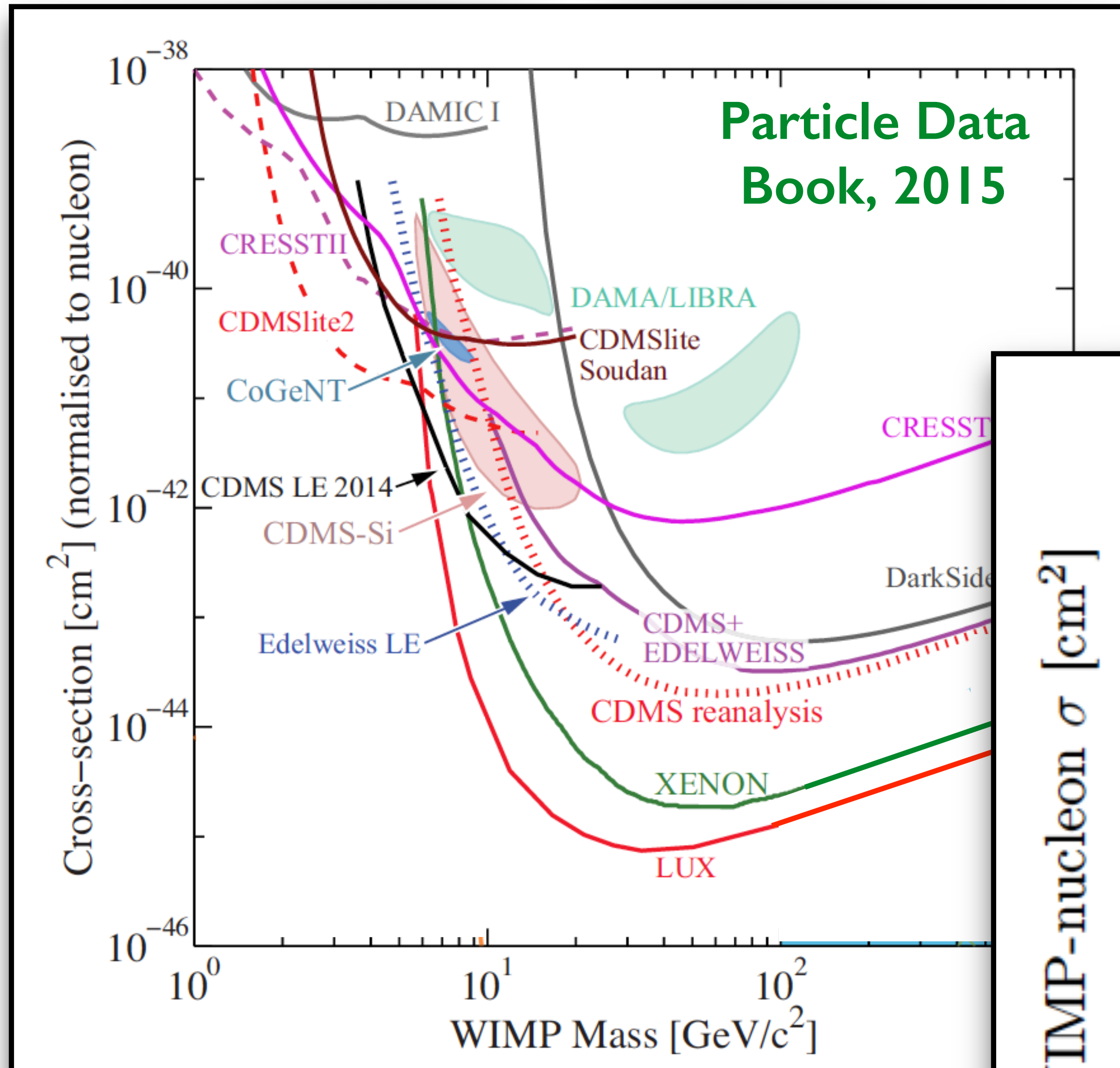

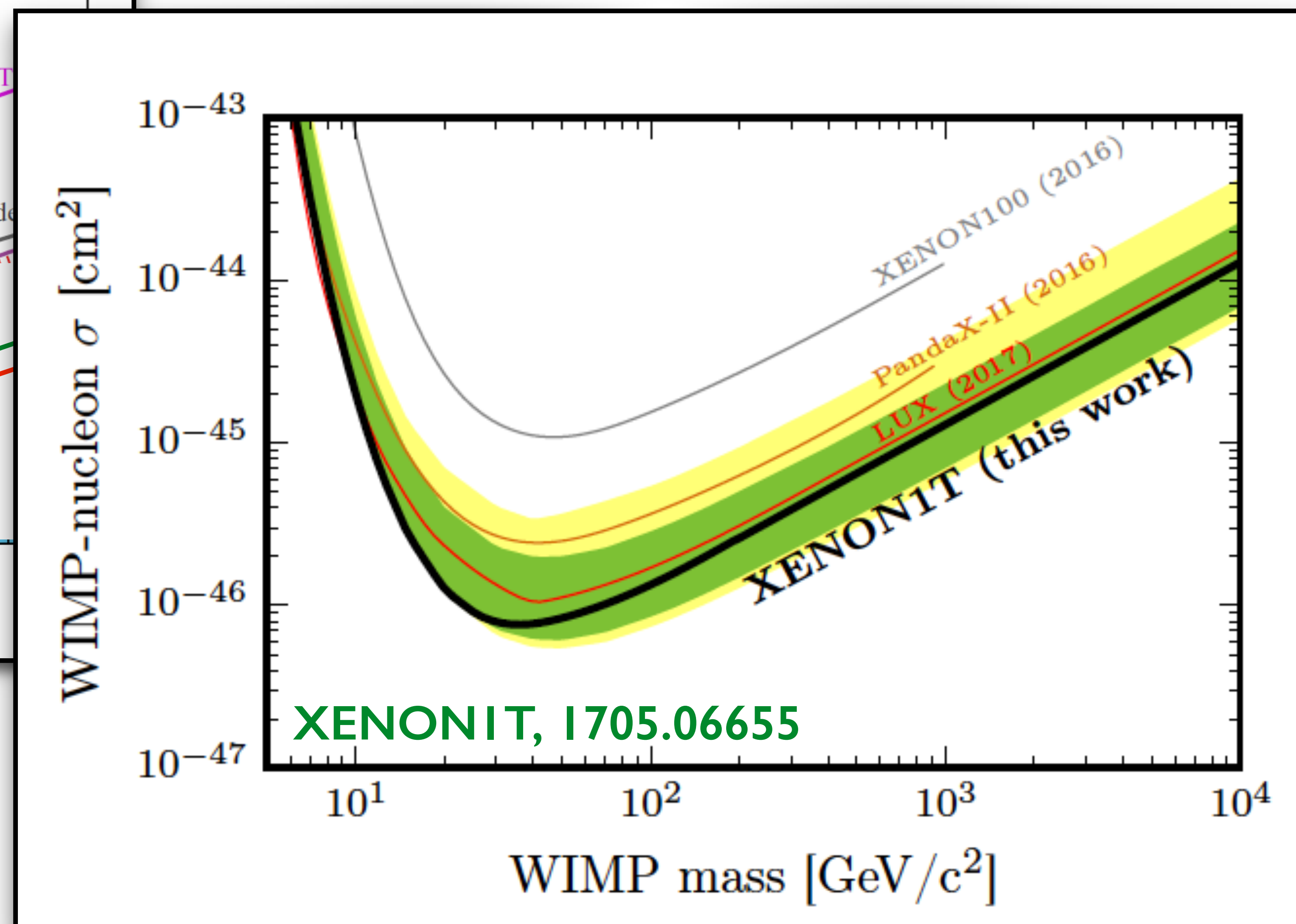

- Assumption in these kinds of plots: **Standard Halo Model**

Local Dark Matter density

From observations:

- **Local estimates:** use kinematical data from a nearby population of stars.
  - Robust measurements, but need to account for the local contribution of baryons which has significant uncertainties. → *large error bars*

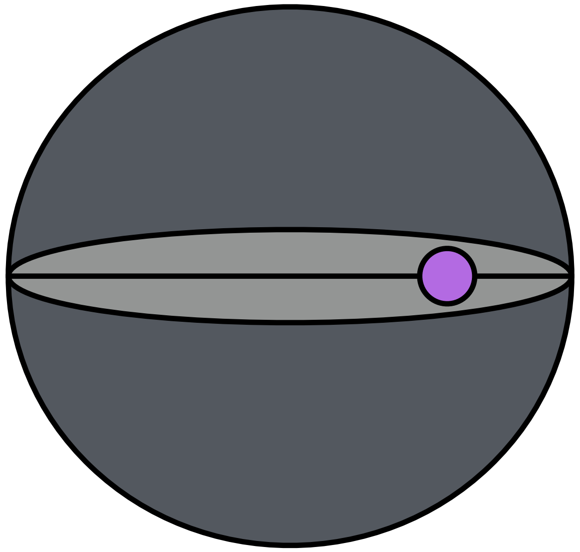

Local Dark Matter density

From observations:

- **Local estimates:** use kinematical data from a nearby population of stars.
  - Robust measurements, but need to account for the local contribution of baryons which has significant uncertainties. → *large error bars*

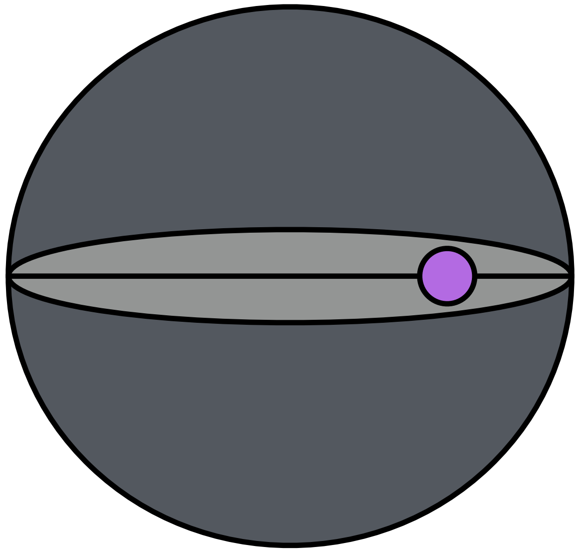

- **Global estimates:** based on mass modeling of the Milky Way (MW), and fits to kinematical data across the Galaxy.
  - Good precision (~10%), but estimates are strongly model dependent. → *systematic uncertainties*

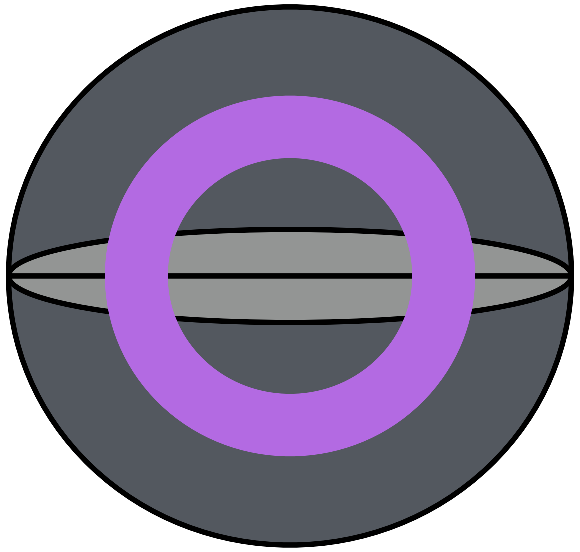

Local Dark Matter density

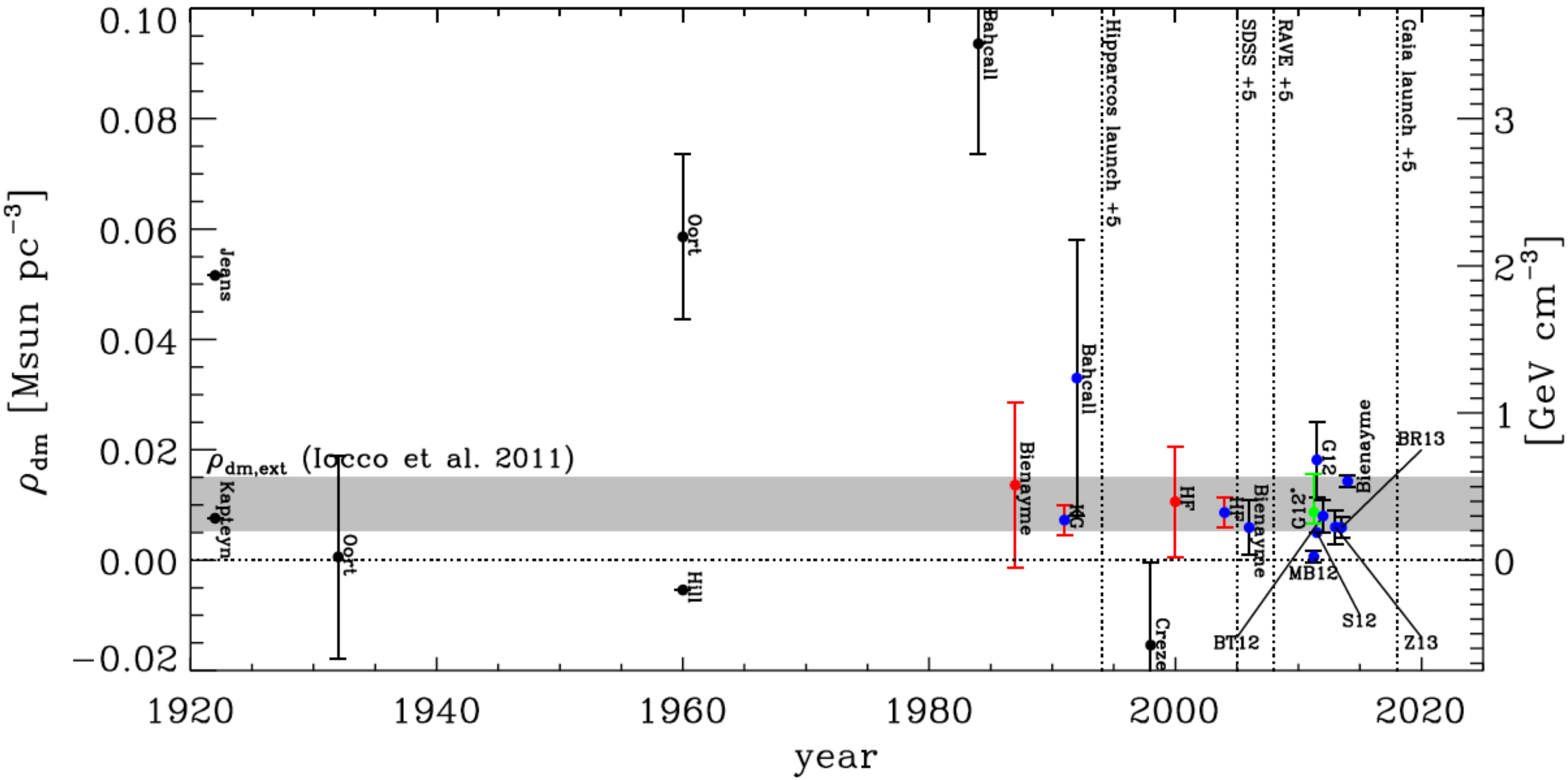

Read, 1404.1938

Local DM velocity distribution

- The velocity distribution depends on the halo model.
- In the **SHM**, a truncated Maxwellian velocity distribution is assumed:

$$f_{\rm gal}(\mathbf{v}) = \begin{cases} N \exp\left(-\mathbf{v}^2/v_c^2\right) & v < v_{\rm esc} \\ 0 & v \geq v_{\rm esc} \end{cases}$$

with $v_c = 220~\mathrm{km/s}$ and $v_{\rm esc} = 550~\mathrm{km/s}$.
$\sigma_v = \sqrt{3/2}~v_c$ independent of radius.

Local DM velocity distribution

- The velocity distribution depends on the halo model.
- In the **SHM**, a truncated Maxwellian velocity distribution is assumed:

$$f_{\rm gal}(\mathbf{v}) = \begin{cases} N \exp\left(-\mathbf{v}^2/v_c^2\right) & v < v_{\rm esc} \\ 0 & v \geq v_{\rm esc} \end{cases}$$

with $v_c = 220\ \mathrm{km/s}$ and $v_{\rm esc} = 550\ \mathrm{km/s}$.
$\sigma_v = \sqrt{3/2}\, v_c$ independent of radius.

- What can we learn from numerical simulations of galaxy formation about the local DM velocity distribution?

Dark Matter only simulations

- DM speed distributions from cosmological N-body simulations **without baryons**, deviate substantially from a Maxwellian.

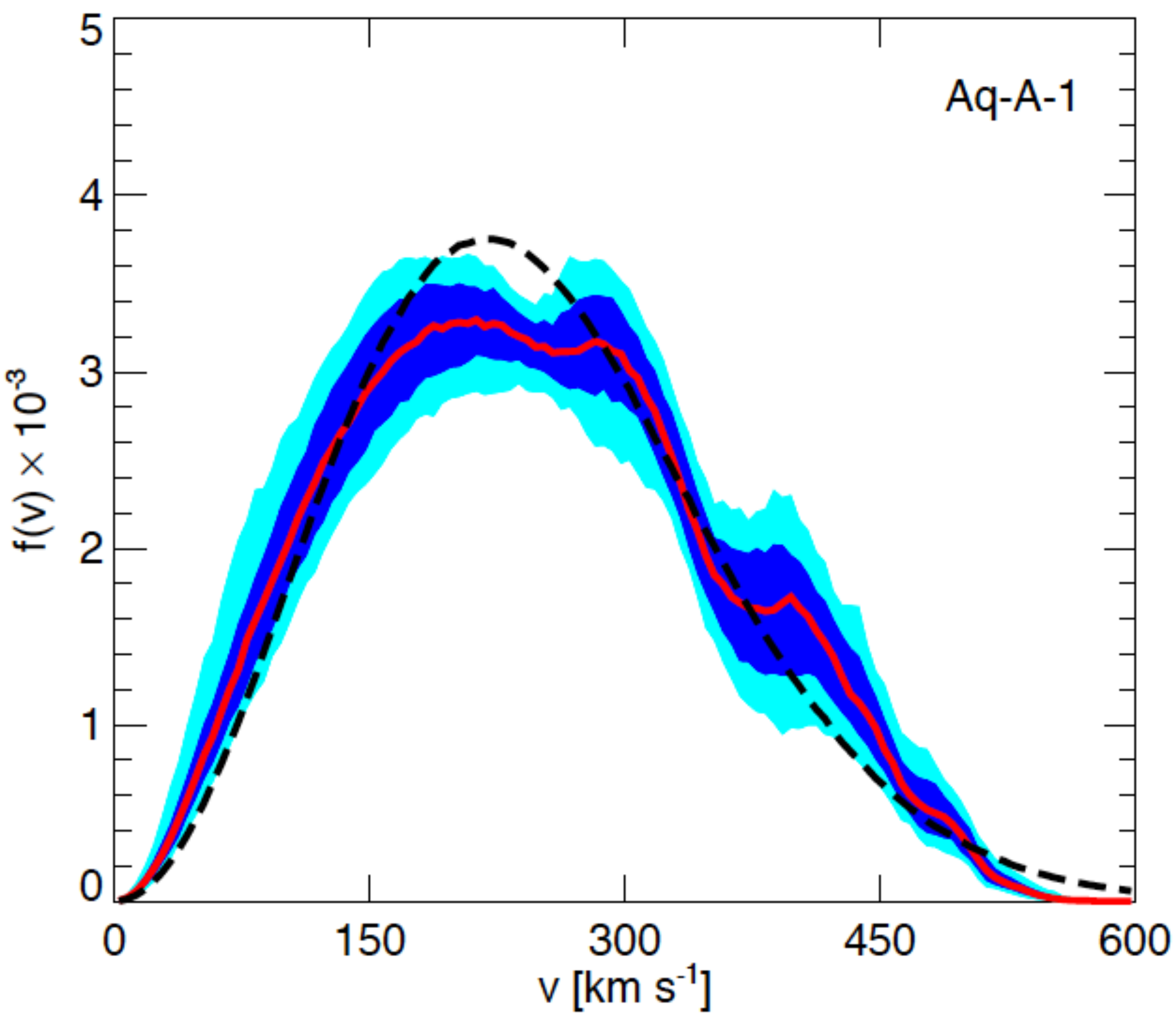

$$f(|\mathbf{v}|) = v^2 \int d\Omega_{\mathbf{v}} f(\mathbf{v})$$

Vogelsberger et al., 0812.0362

- *Significant systematic uncertainty since the impact of baryons neglected.*

Hydrodynamical simulations

- Each hydrodynamical (**DM + baryons**) simulation adopts a different *galaxy formation model*, *spatial resolution*, *DM particle mass*.

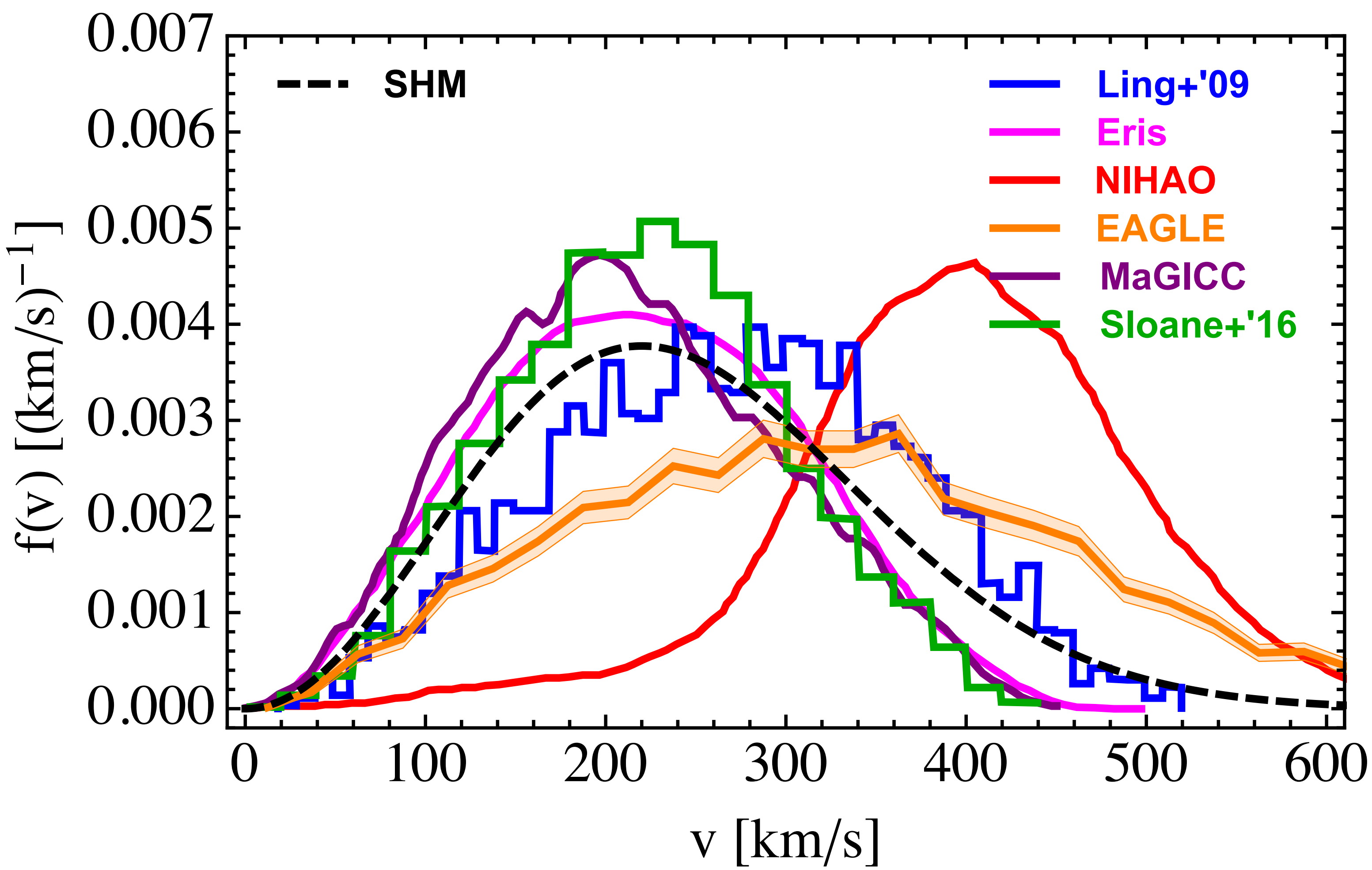

Bozorgnia & Bertone, 1705.05853

- Large variation in DM speed distributions between the results of different simulations.

Hydrodynamical simulations

- Each hydrodynamical (**DM + baryons**) simulation adopts a different *galaxy formation model*, *spatial resolution*, *DM particle mass*.

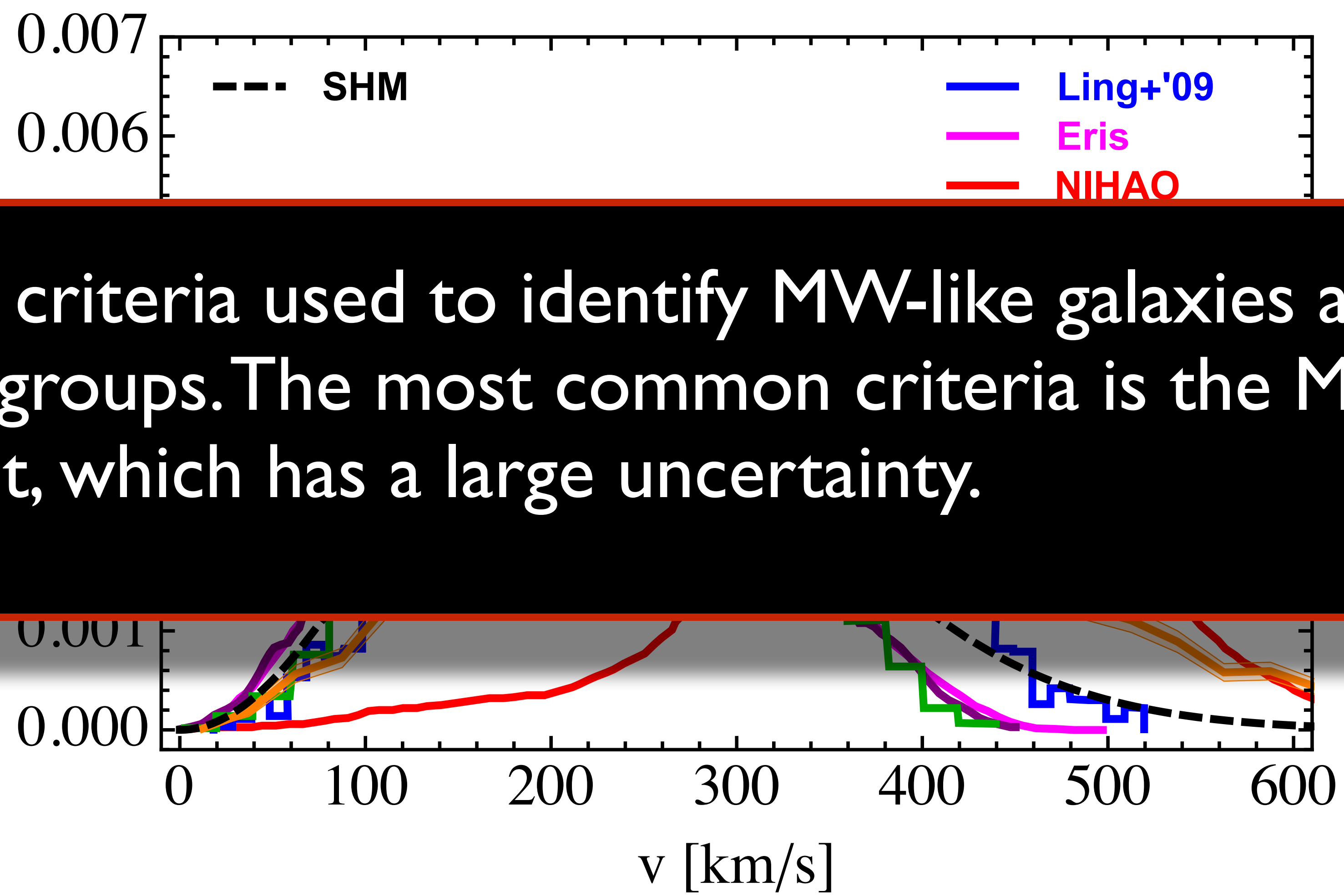

Different criteria used to identify MW-like galaxies among different groups. The most common criteria is the MW mass constraint, which has a large uncertainty.

Bozorgnia & Bertone, 1705.05853

- Large variation in DM speed distributions between the results of different simulations.

Hydrodynamical simulations

- To make precise quantitative predictions:
  - Model baryonic processes in a way that the main galaxy population properties are broadly reproduced.
  - Identify MW-like galaxies by taking into account observational constraints on the MW.

Hydrodynamical simulations

- To make precise quantitative predictions:
  - Model baryonic processes in a way that the main galaxy population properties are broadly reproduced.
  - Identify MW-like galaxies by taking into account observational constraints on the MW.
- We use the **EAGLE** and **APOSTLE** hydrodynamic simulations. *calibrated to reproduce the observed distribution of stellar masses and sizes of low-redshift galaxies.*
- Companion Dark Matter only (DMO) simulations were run assuming all the matter content is collisionless.

EAGLE Simulations

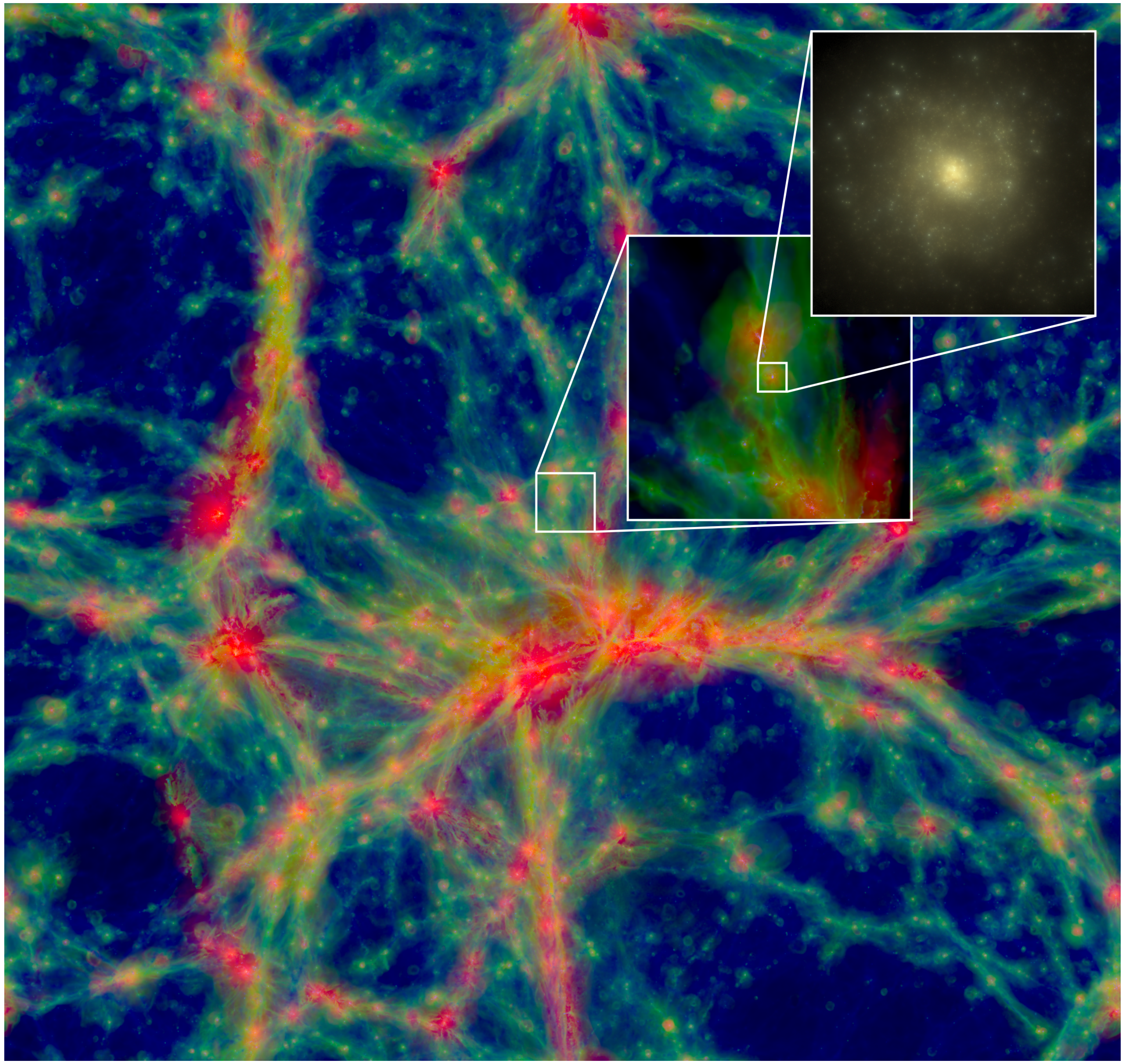

EAGLE Simulations, 1407.7040

Milky Way analogues

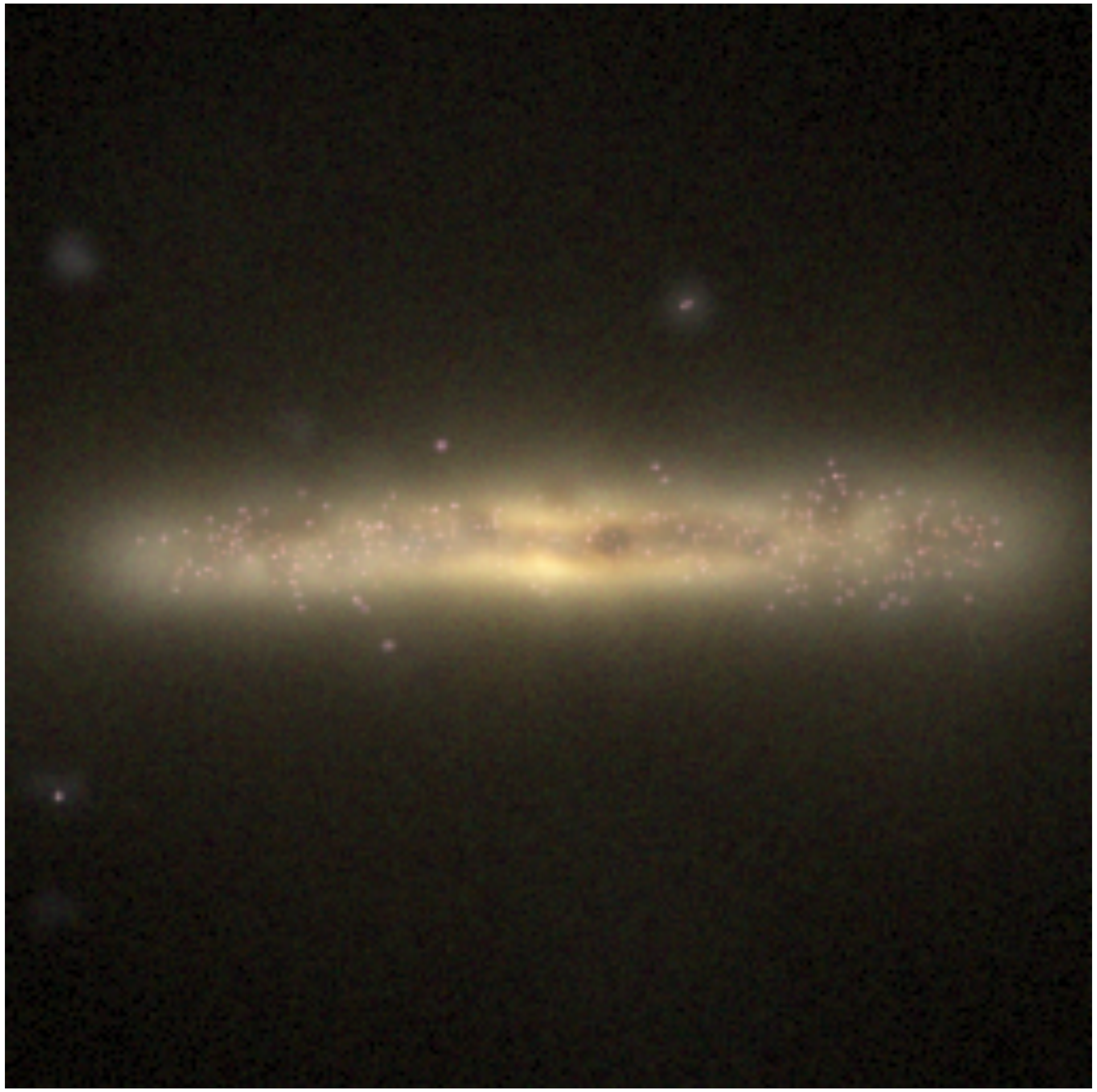

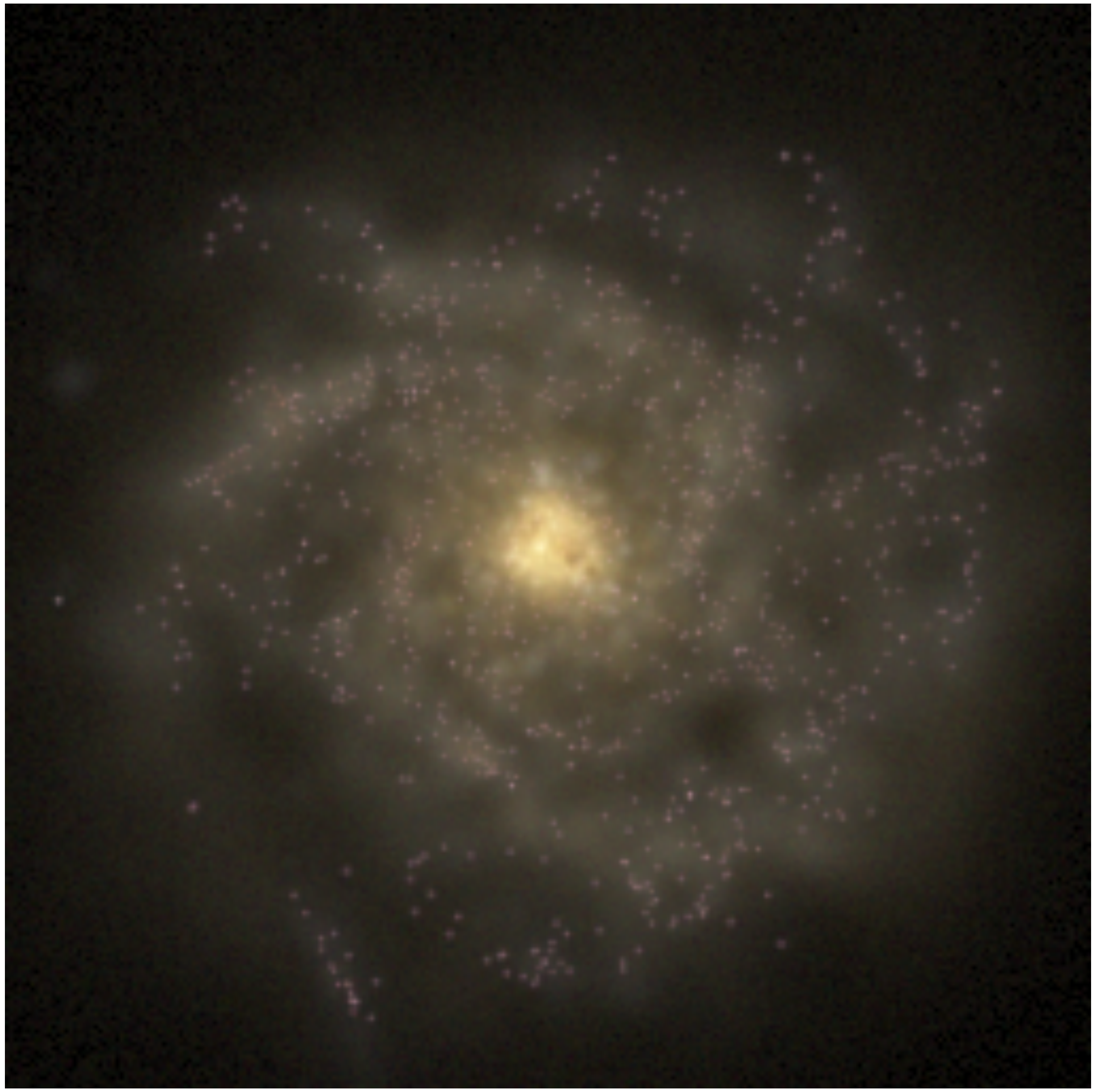

Identifying Milky Way analogues

- We introduce new criteria to identify MW analogues using observed MW kinematical data: **rotation curves, total stellar mass.**

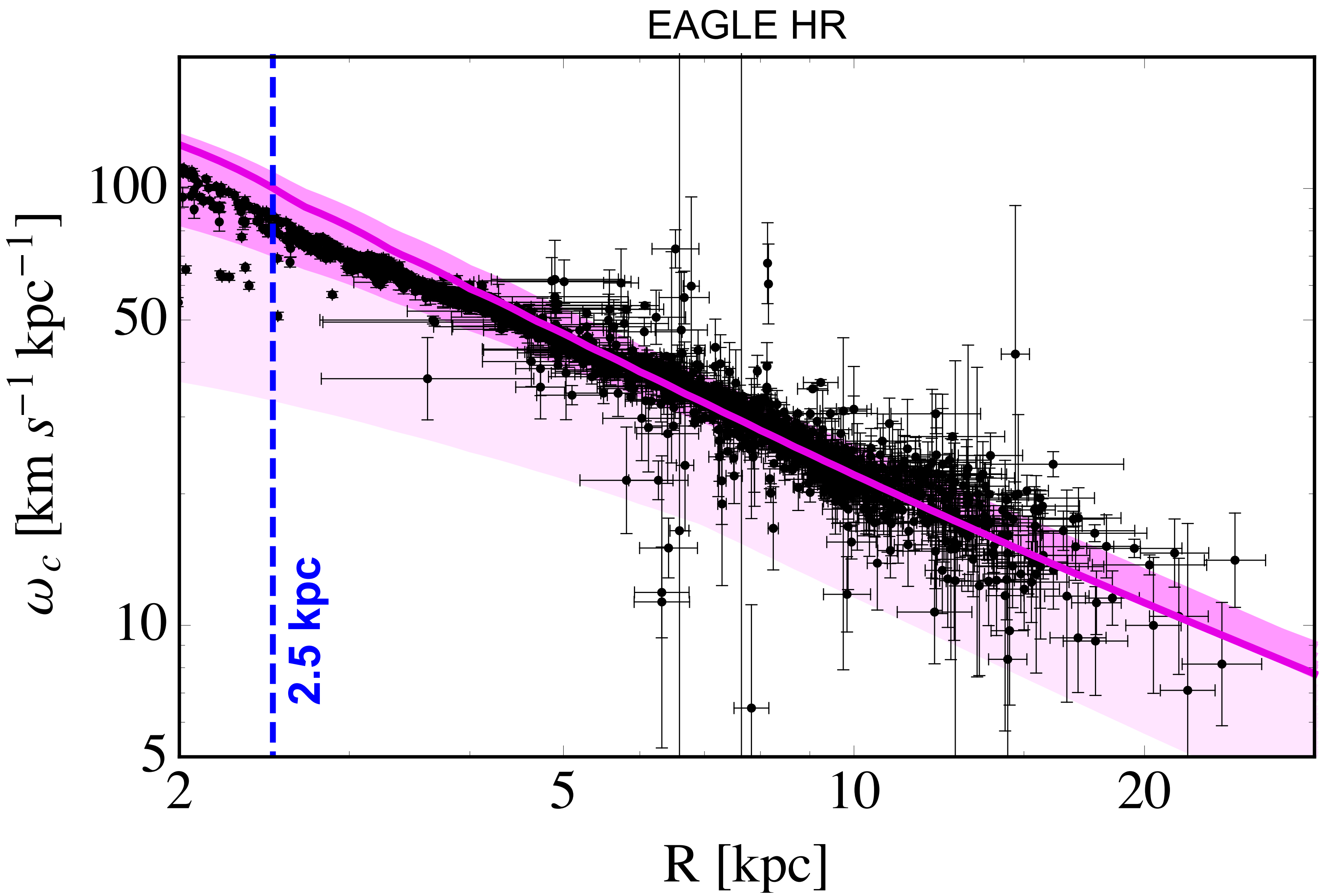

14 MW analogues

Bozorgnia et al., 1601.04707
Calore, Bozorgnia et al., 1509.02164

Dark Matter density profiles

- Spherically averaged DM density profiles of the MW analogues:

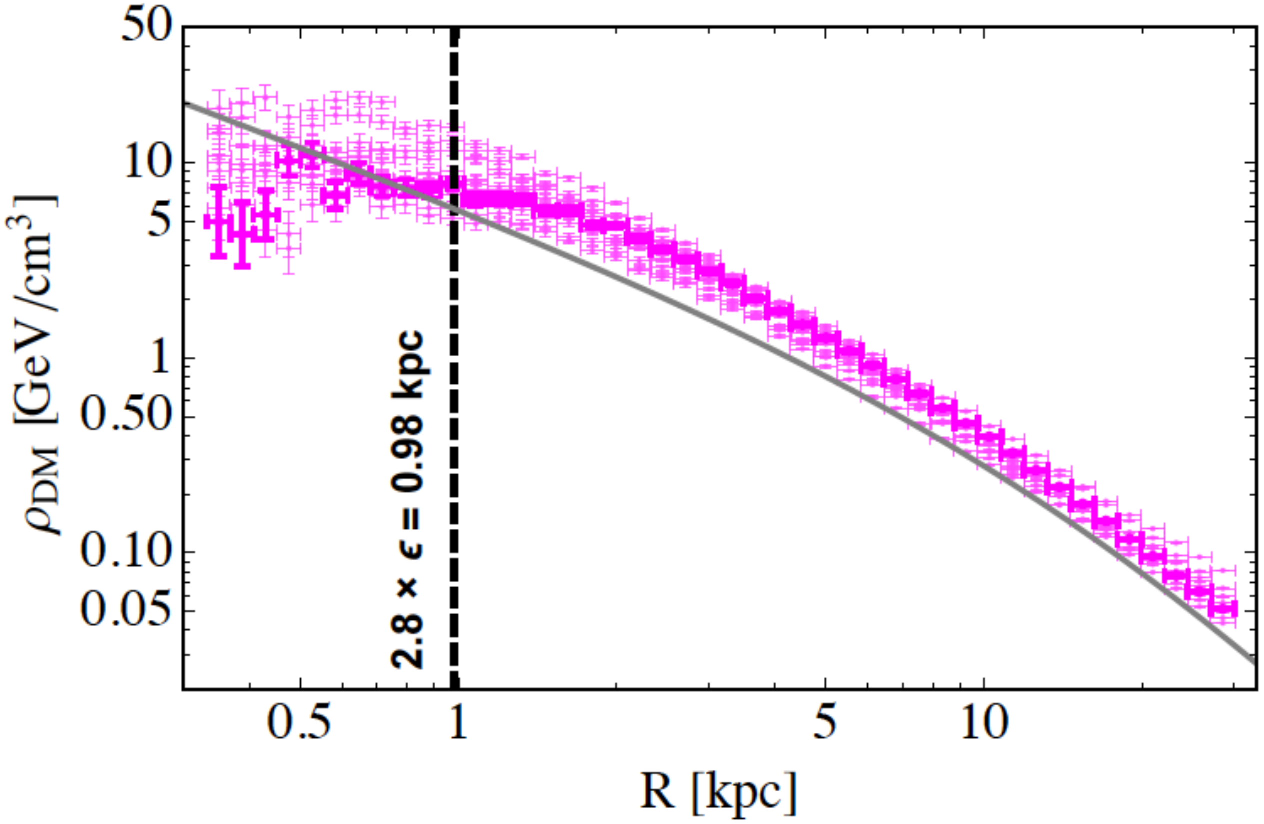

Dark Matter density profiles

- Spherically averaged DM density profiles of the MW analogues:

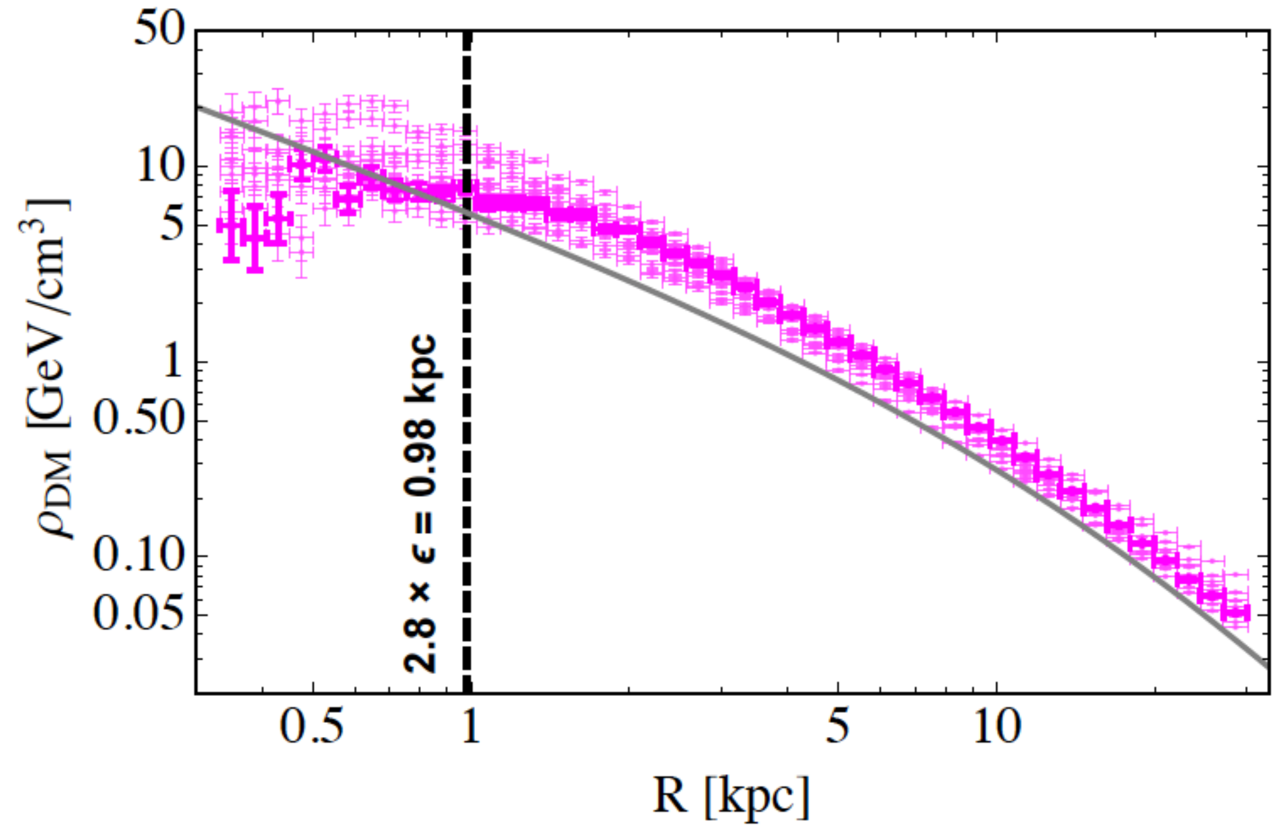

- To find the DM density at the position of the Sun, consider a torus aligned with the stellar disc.

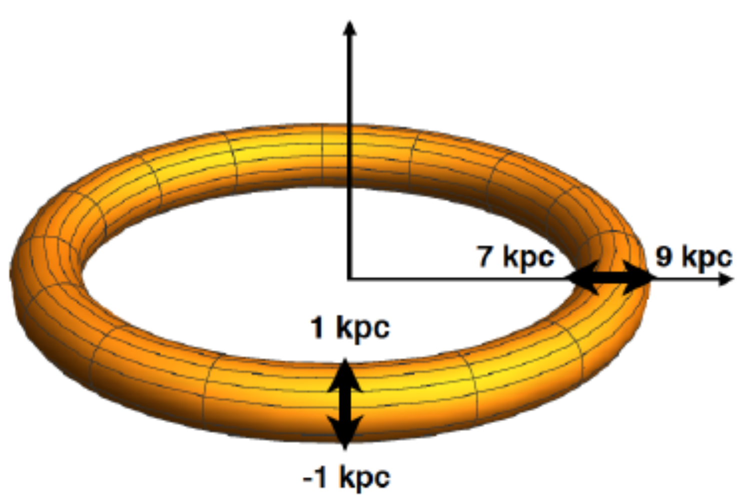

$$\rho_\chi = 0.41 - 0.73 \text{ GeV/cm}^3$$

Bozorgnia et al., 1601.04707

Local speed distributions

In the galactic rest frame:

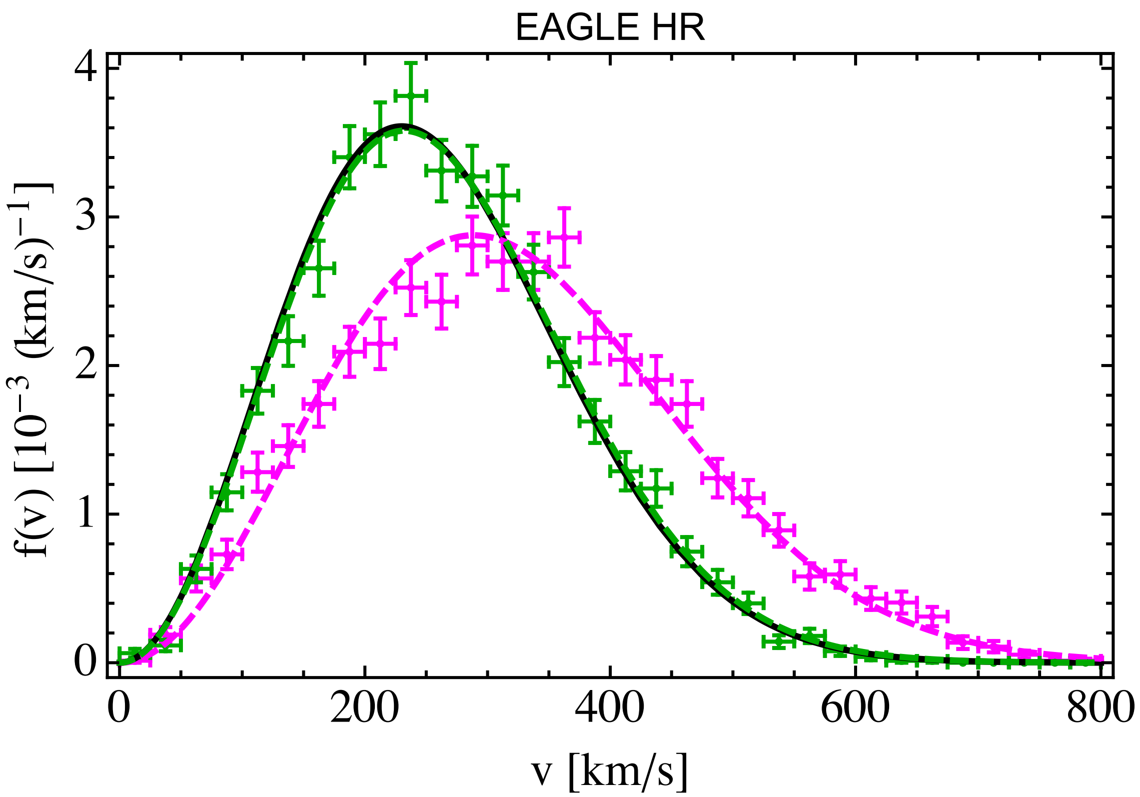

DMO simulations

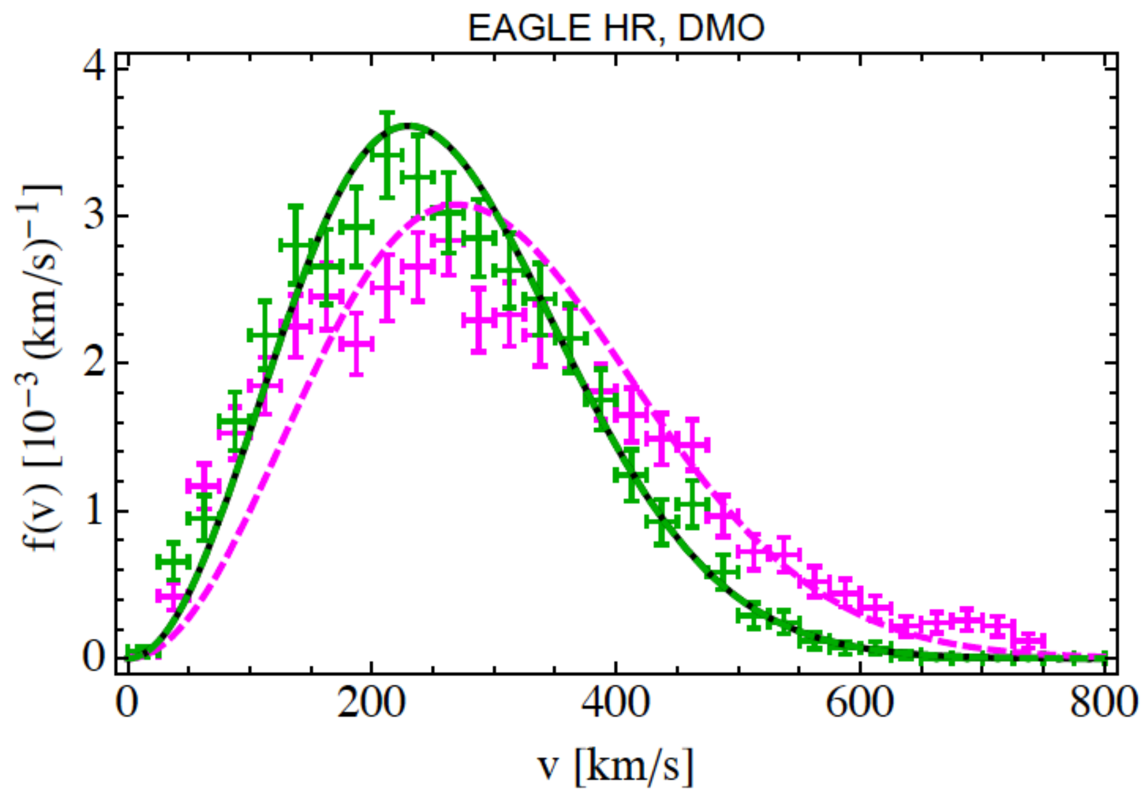

Bozorgnia et al., 1601.04707

Local speed distributions

In the galactic rest frame:

DMO simulations

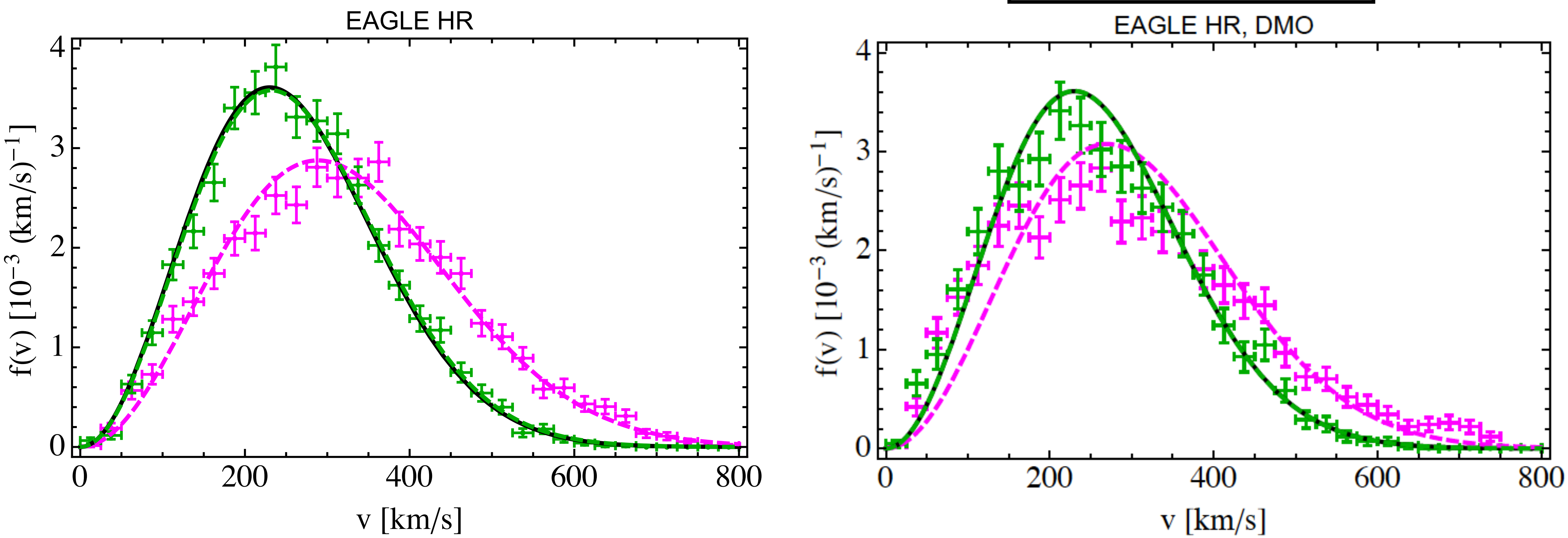

Bozorgnia et al., 1601.04707

- Maxwellian distribution with a free peak provides a better fit to haloes in the hydrodynamical simulations compared to their DMO counterparts.
- Best fit peak speed: v_{peak} = 223 - 289 km/s

Local speed distributions

Common trends in different hydrodynamical simulations:

- Baryons deepen the gravitational potential in the inner halo, shifting the peak of the DM speed distribution to *higher speeds.*
- In most cases, baryons appear to make the local DM speed distribution ***more Maxwellian***.

Bozorgnia & Bertone, 1705.05853

Components of the velocity distribution

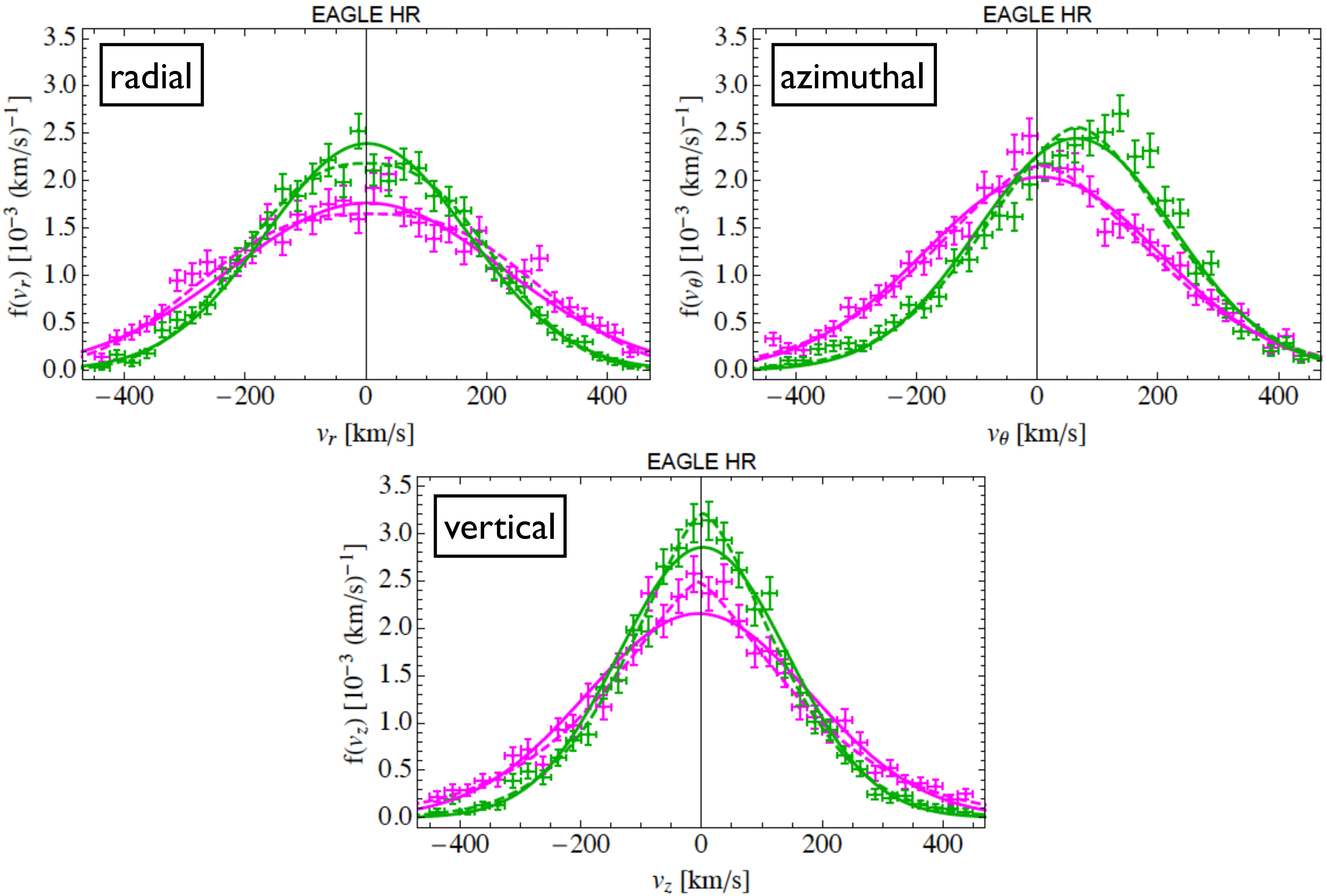

Bozorgnia et al., 1601.04707

How common are dark disks?

- Clear velocity anisotropy at the Solar circle.
- Two haloes have a rotating DM component in the disc with mean velocity comparable (within 50 km/s) to that of the stars.

How common are dark disks?

- Clear velocity anisotropy at the Solar circle.
- Two haloes have a rotating DM component in the disc with mean velocity comparable (within 50 km/s) to that of the stars.
- Hint for the existence of a co-rotating dark disk in 2 out of 14 MW-like haloes. → **Dark disks are relatively rare in our halo sample.**

Bozorgnia et al., 1601.04707
Schaller et al., 1605.02770

How common are dark disks?

- Clear velocity anisotropy at the Solar circle.
- Two haloes have a rotating DM component in the disc with mean velocity comparable (within 50 km/s) to that of the stars.
- Hint for the existence of a co-rotating dark disk in 2 out of 14 MW-like haloes. → **Dark disks are relatively rare in our halo sample.**

Bozorgnia et al., 1601.04707
Schaller et al., 1605.02770

- *Sizable dark disks also rare in other hydro simulations:*
    - They only appear in simulations where a large satellite merged with the MW in the recent past, which is robustly excluded from MW kinematical data.

Bozorgnia & Bertone, 1705.05853

The halo integral

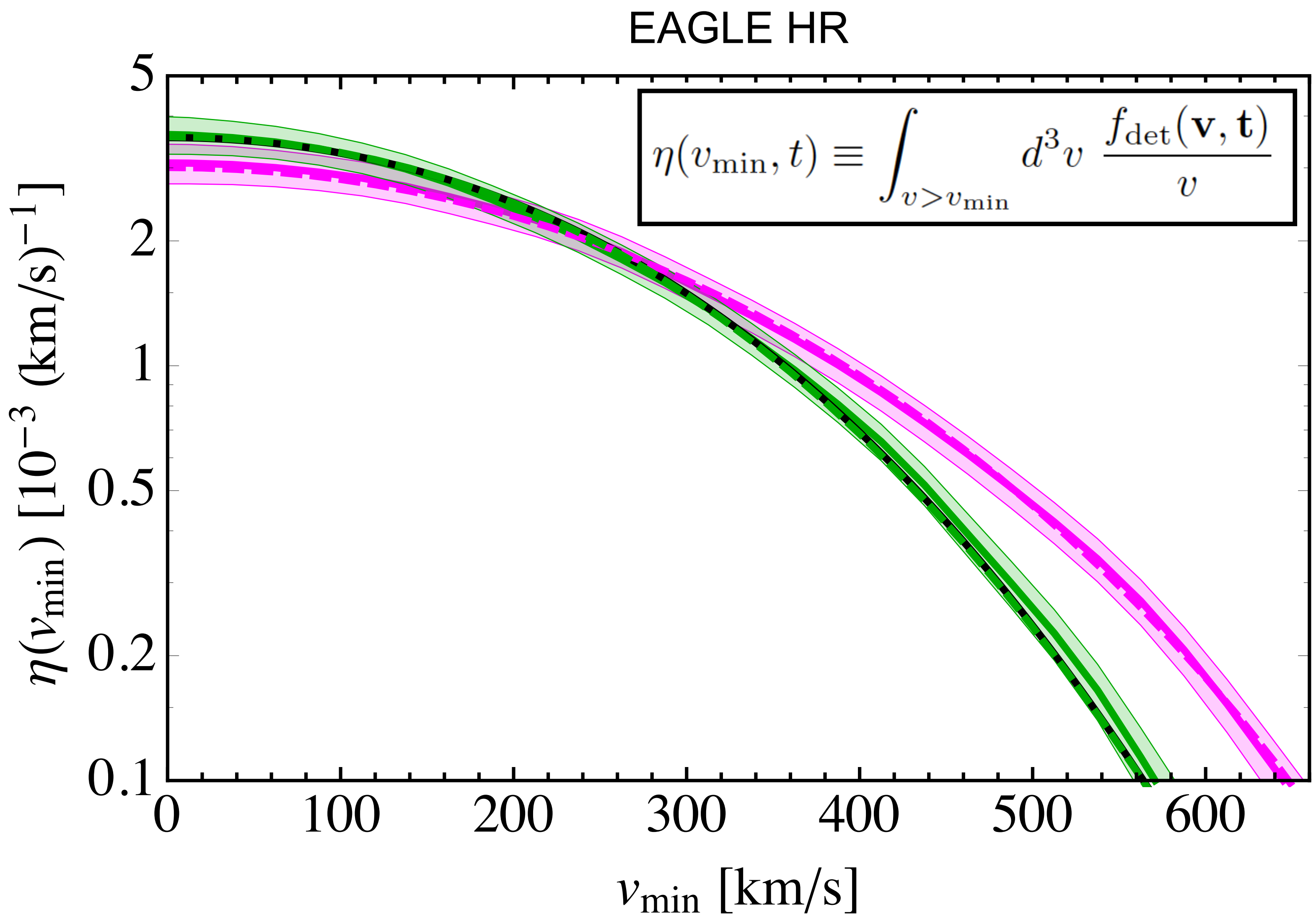

- Halo integrals for the best fit Maxwellian velocity distribution (*peak speed 223 - 289 km/s*) fall within the 1σ uncertainty band of the halo integrals of the simulated haloes.

Bozorgnia et al., 1601.04707

The halo integral

Common trend in different hydrodynamical simulations:

- Halo integrals and hence direct detection event rates obtained from a Maxwellian velocity distribution with a free peak are similar to those obtained directly from the simulated haloes.

Bozorgnia et al., 1601.04707 (EAGLE & APOSTLE)
Kelso et al., 1601.04725 (MaGICC)
Sloane et al., 1601.05402
Bozorgnia & Bertone, 1705.05853

Implications for direct detection

- Assuming the **Standard Halo Model**:

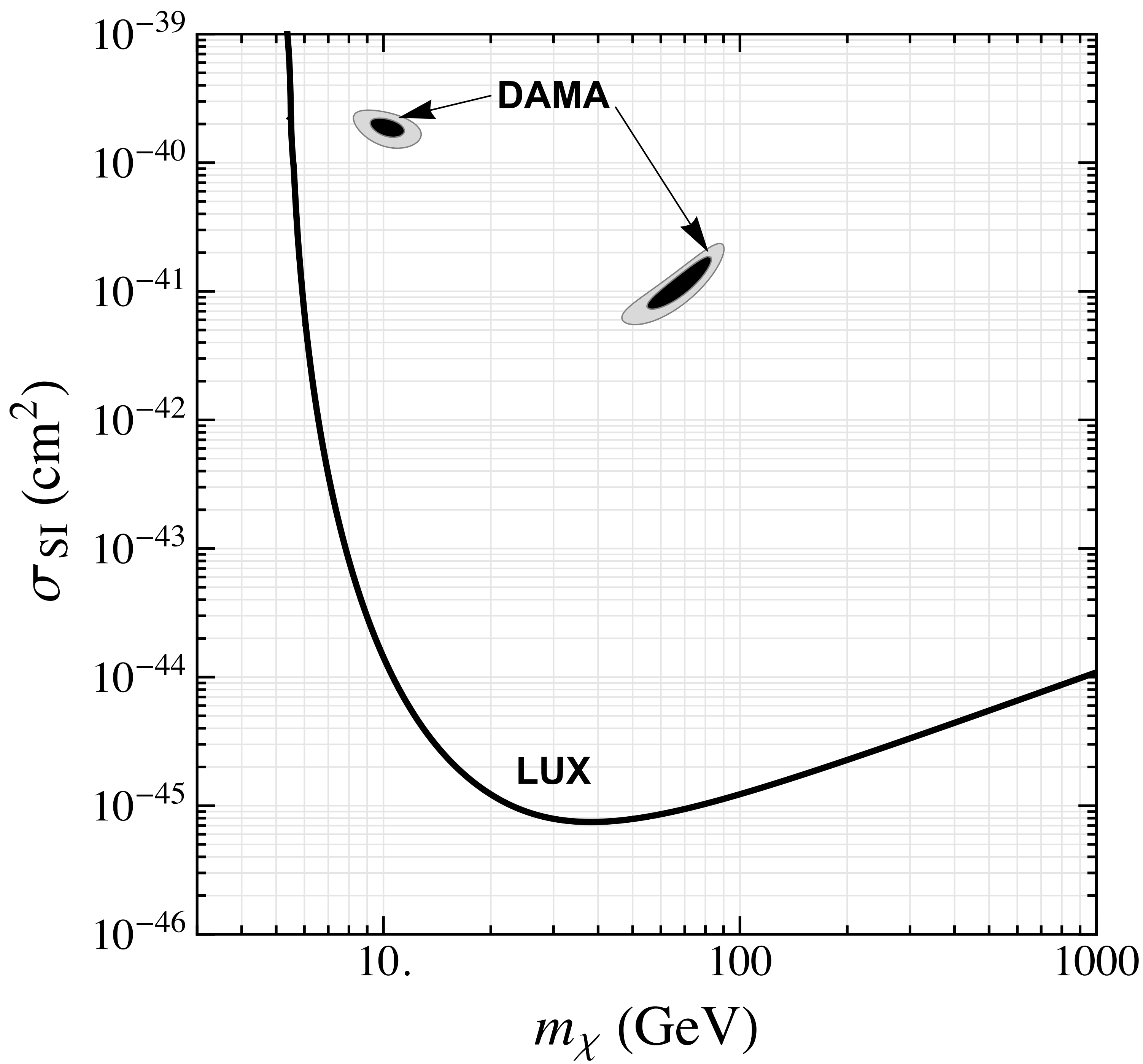

Implications for direct detection

- Compare with simulated Milky Way-like haloes:

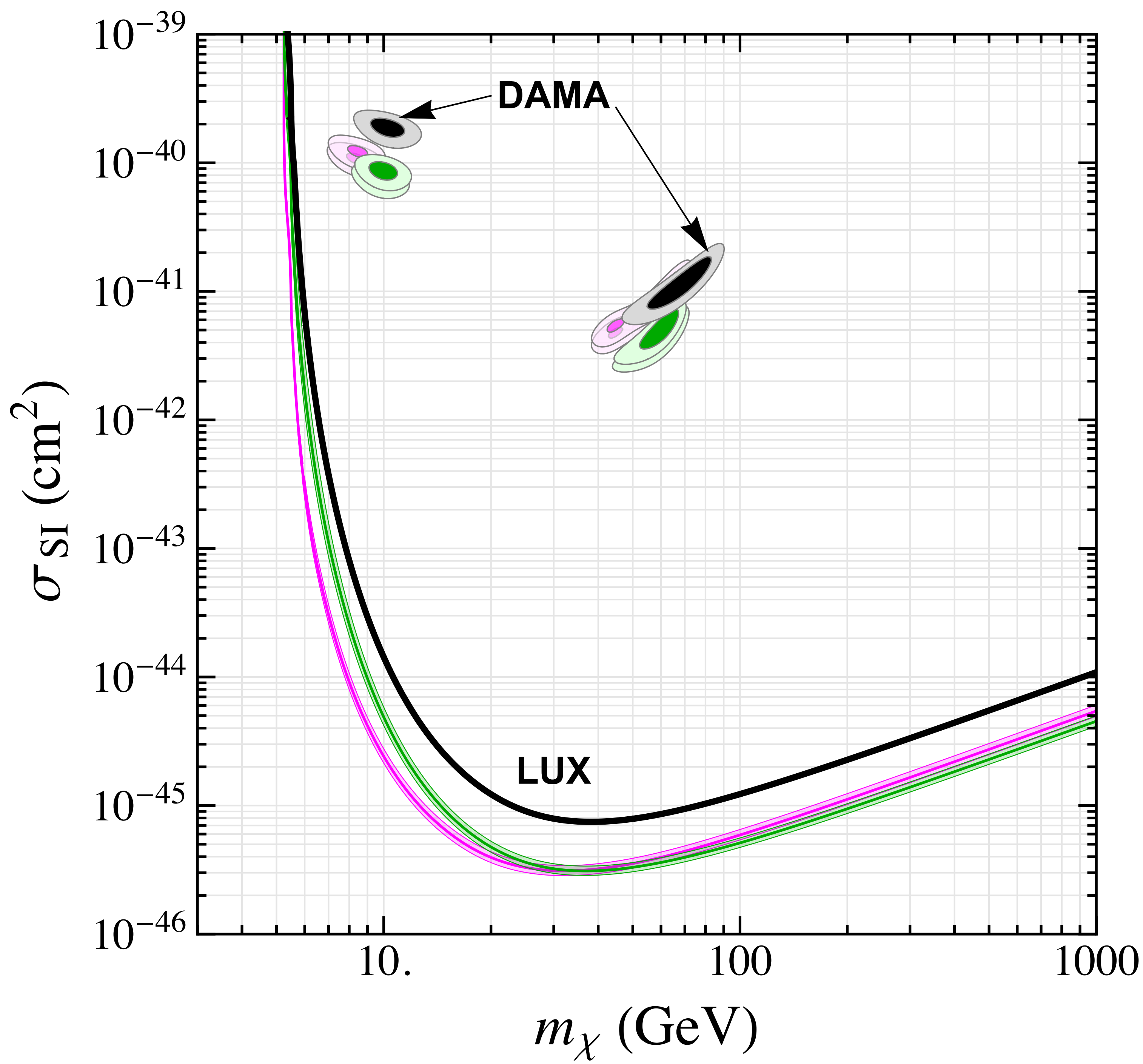

Implications for direct detection

Fix local ρ_χ=0.3 GeV cm^{-3}

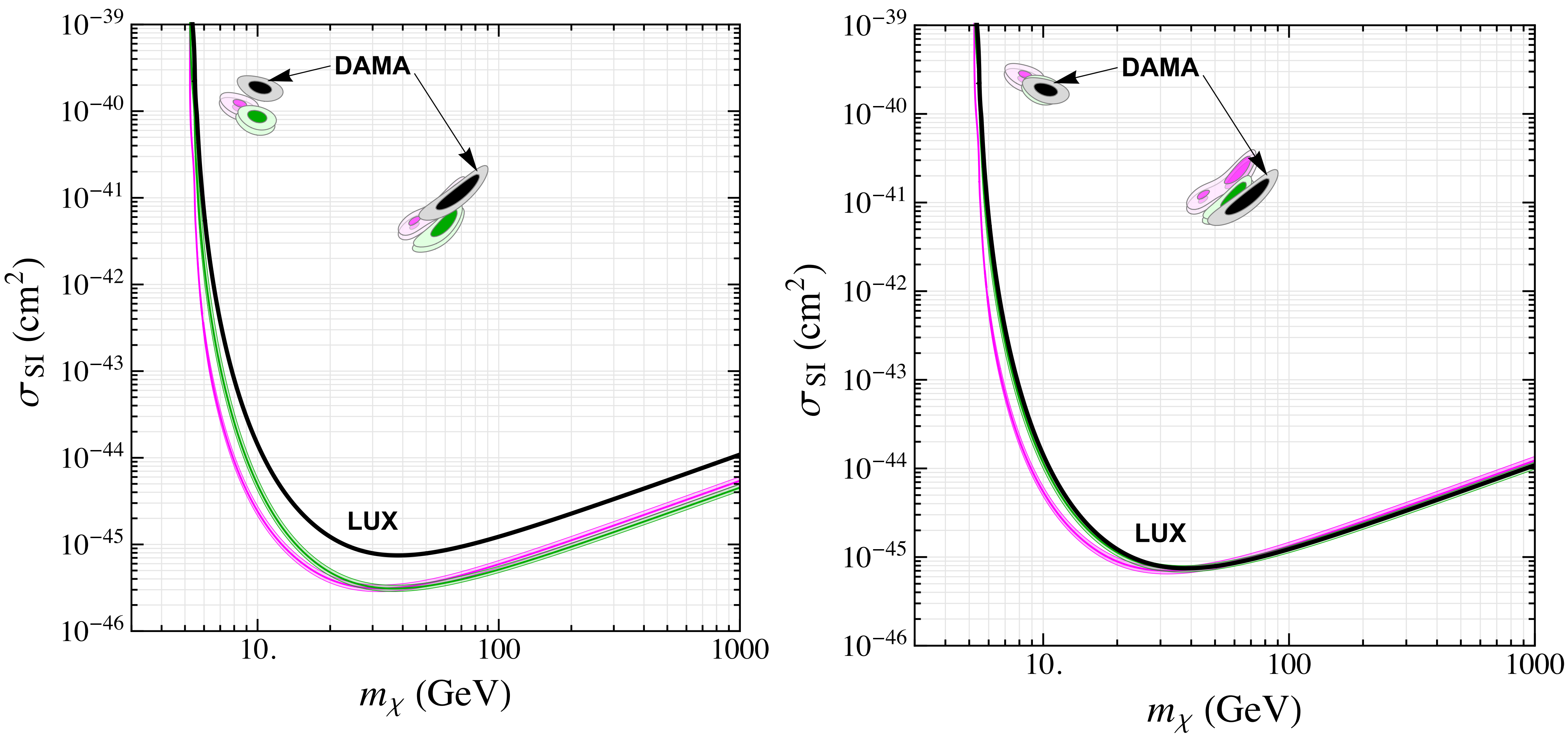

- Difference in the local DM density ➡ overall difference with the SHM.
- Variation in the peak of the DM speed distribution ➡ shift in the low mass region.

Implications for direct detection

Comparison to other hydrodynamical simulations:

Fix local ρ_χ=0.3 GeV cm^{-3}

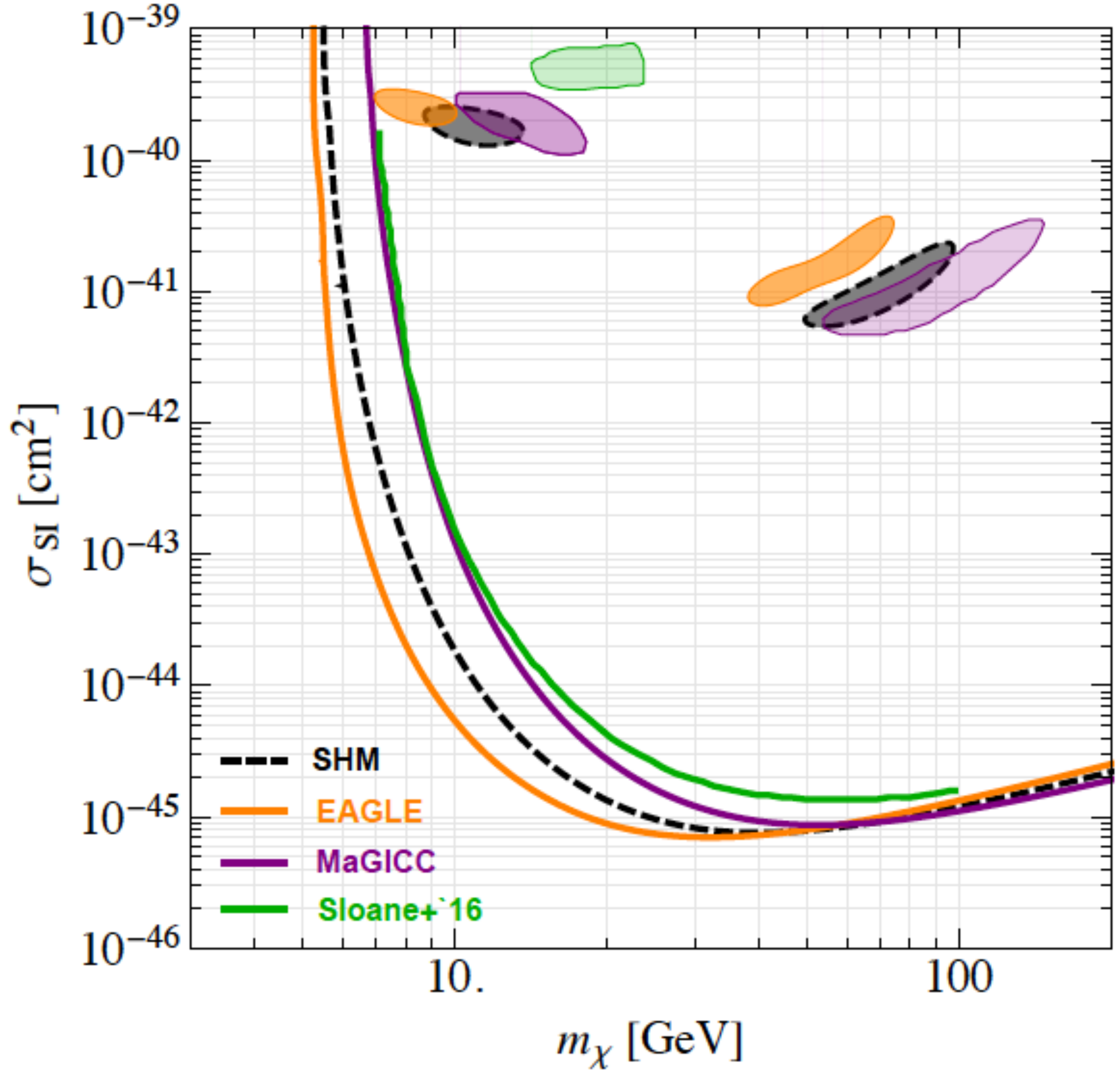

Bozorgnia & Bertone, 1705.05853

Non-standard interactions

- For a very general set of non-relativistic effective operators:

Kahlhoefer & Wild, 1607.04418

$$\frac{d\sigma_{\chi N}}{dE_R} = \frac{d\sigma_1}{dE_R}\frac{1}{v^2} + \frac{d\sigma_2}{dE_R}$$

Non-standard interactions

- For a very general set of non-relativistic effective operators:

Kahlhoefer & Wild, 1607.04418

$$\frac{d\sigma_{\chi N}}{dE_R} = \frac{d\sigma_1}{dE_R}\frac{1}{v^2} + \frac{d\sigma_2}{dE_R}$$

$$\eta(v_{\rm min}, t) \qquad h(v_{\rm min}, t) = \int_{v>v_{\rm min}} d^3v \; v \; f_{\rm det}(\mathbf{v}, t)$$

Non-standard interactions

- For a very general set of non-relativistic effective operators:

Kahlhoefer & Wild, 1607.04418

$$\frac{d\sigma_{\chi N}}{dE_R} = \frac{d\sigma_1}{dE_R}\frac{1}{v^2} + \frac{d\sigma_2}{dE_R}$$

$$\eta(v_{\rm min}, t) \qquad h(v_{\rm min}, t) = \int_{v>v_{\rm min}} d^3v \; v \; f_{\rm det}(\mathbf{v}, t)$$

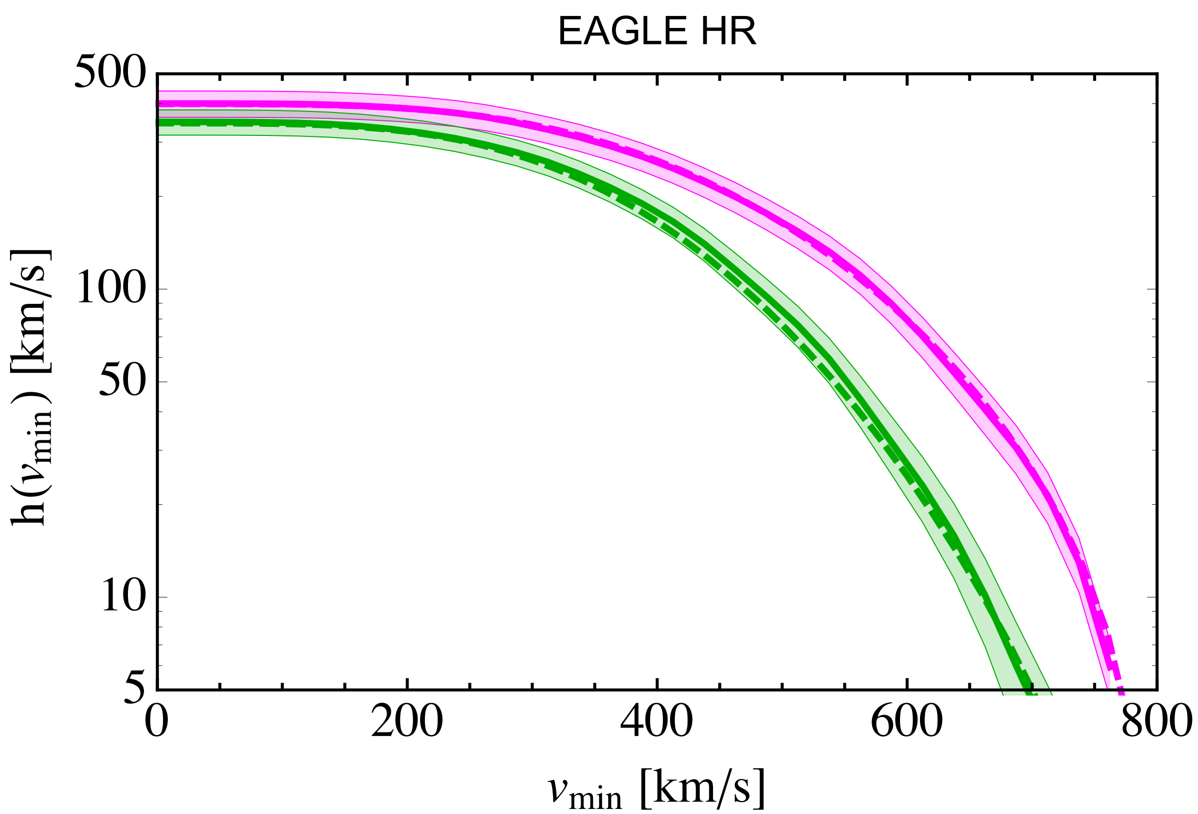

Bozorgnia & Bertone, 1705.05853

- Best fit Maxwellian $h(v_{\rm min})$ falls within the 1σ uncertainty band of the $h(v_{\rm min})$ of the simulated haloes.

Summary

- Need *a precise determination of the local DM distribution in the MW* to accurately determine the DM particle physics properties.

- Extract the DM distribution from cosmological simulations.
  → *Identify MW analogues* by taking into account observational constraints on the MW.

  - **Local DM density** agrees with local and global estimates.

  - **Halo integrals** of MW analogues match well those obtained from best fit Maxwellian velocity distribution.

- A Maxwellian velocity distribution with *peak speed* constrained by hydro simulations, and independent from the *local circular speed*, could be used for the analysis of direct detection data.

Backup Slides

Observations vs. simulations

Goodness of fit to the observed data:

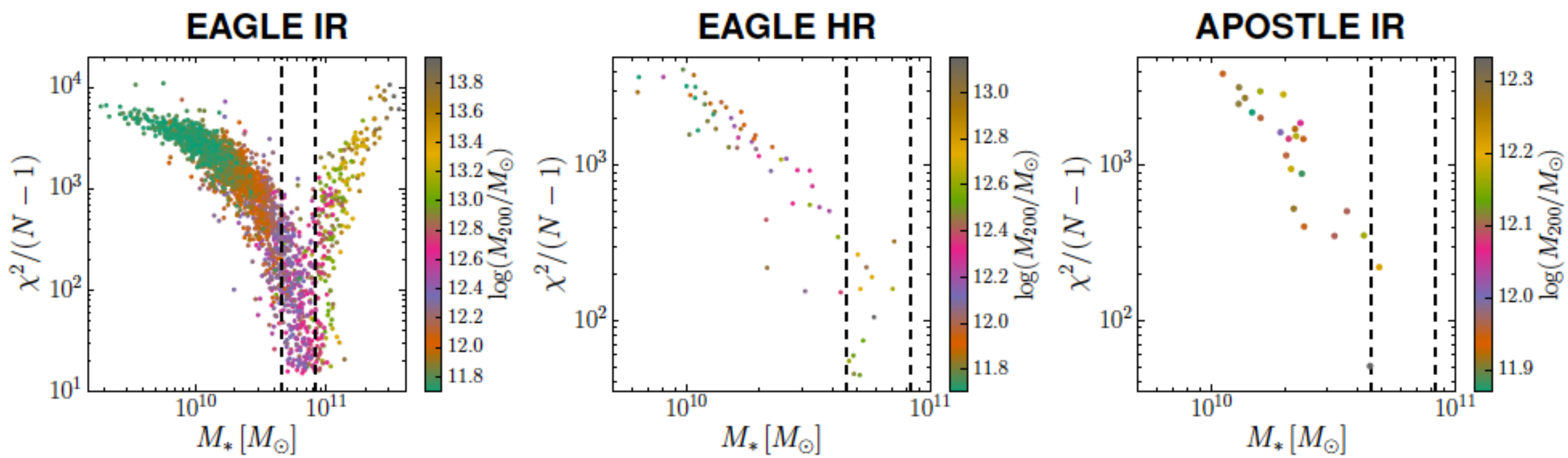

$N = 2687$ is the total number of observational data points used.

- Minimum of the reduced χ^2 occurs within the 3σ measured range of the MW total stellar mass. $\Rightarrow$ haloes with correct MW stellar mass have rotation curves which match well the observations.
- We focus only on the selected **EAGLE HR** and **APOSTLE IR** haloes due to higher resolution $\Rightarrow$ total of **14** MW analogues.

Selection criteria for MW analogues

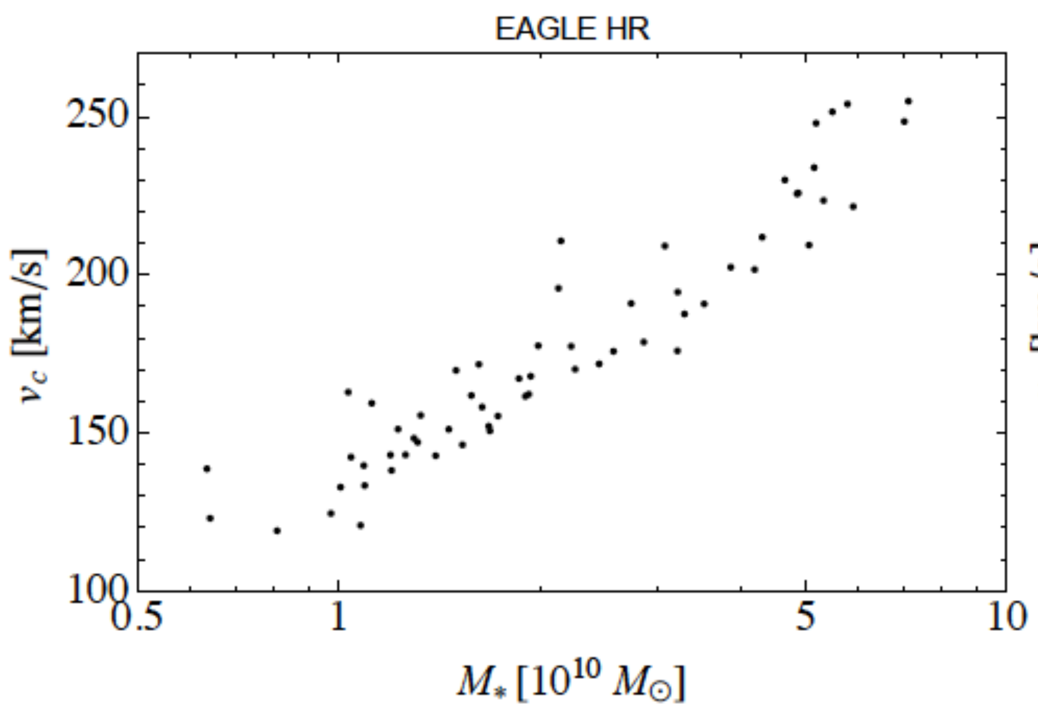

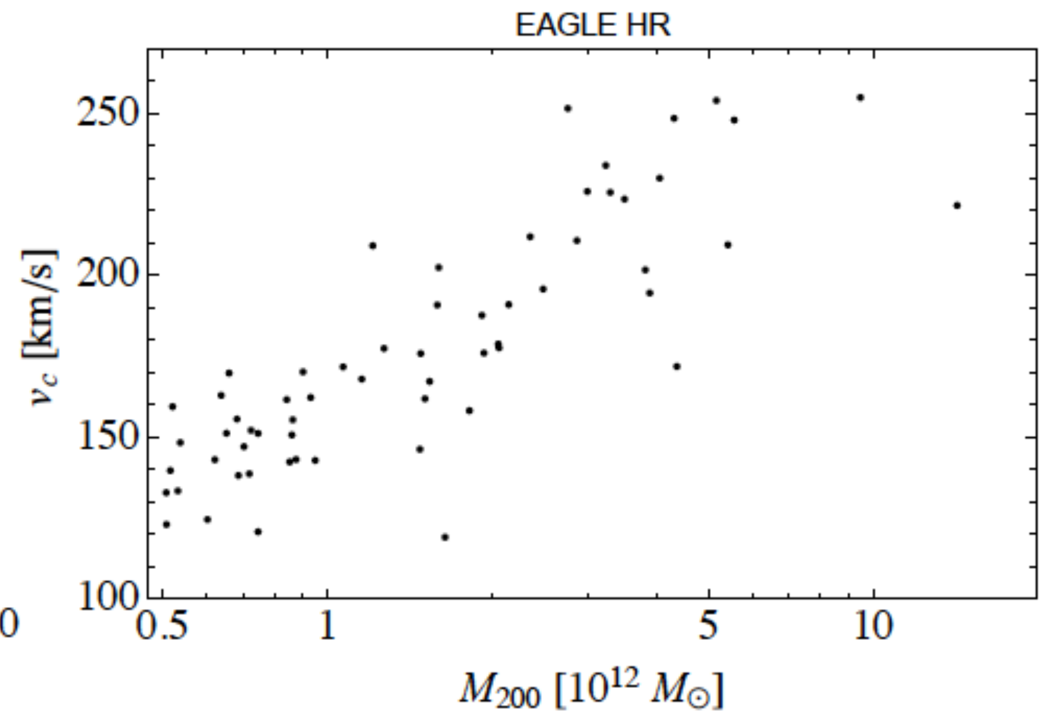

- $M_\star$ strongly correlated with v_c at 8 kpc, while the correlation of M_{200} with v_c is weaker.
- $M_\star(R < 8 \text{ kpc}) = (0.5 - 0.9)M_\star$.
- $M_{\text{tot}}(R < 8 \text{ kpc}) = (0.01 - 0.1)M_{200}$.
- Over the small halo mass range probed, little correlation between $M_{\text{DM}}(R < 8 \text{ kpc})$ and M_{200}.

Searching for dark disks

DM and stellar velocity distributions:

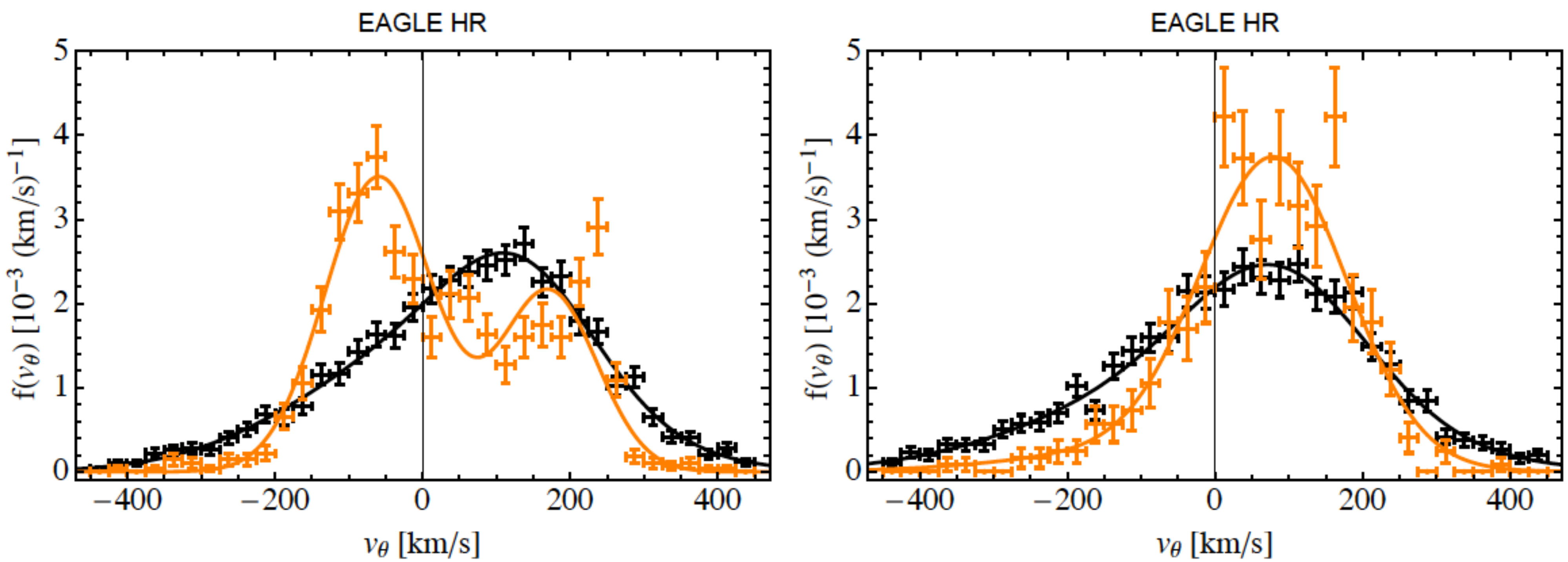

- Fit with a double Gaussian. Difference in the mean speed of second Gaussian between DM and stars is 35 km/s in the left, and 7 km/s in the right panel.
- Fraction of second Gaussian is 32% in the left panel and 43% in the right panel.

Searching for dark disks

Is there an enhancement of the local DM density in the **Galactic disc** compared to the **halo**?

- Compare the the average $\rho_{\rm DM}$ in the torus with the value in a spherical shell at $7 < R < 9$ kpc.

  $\rho_{\rm DM}^{\rm torus}$ is larger than $\rho_{\rm DM}^{\rm shell}$ by:

  2 – 27% for 10 haloes,
  greater than 10% for 5 haloes, and
  greater than 20% for only two haloes.

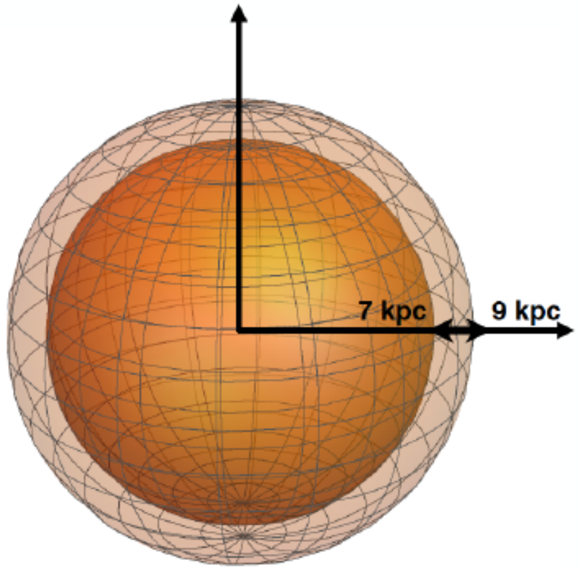

- The increase in the DM density in the disc could be due to the DM halo contraction as a result of dissipational baryonic processes.

Halo shapes

- To study the shape of the inner ($R < 8$ kpc) DM haloes, we calculate the inertia tensor of DM particles within 5 and 8 kpc.
  $\Rightarrow$ ellipsoid with three axes of length $a \geq b \geq c$.

- Calculate the sphericity: $s = c/a$.
  - $s = 1$: perfect sphere. $s < 1$: increasing deviation from sphericity.
  - At 5 kpc, $s = [0.85, 0.95]$. At 8 kpc, s lower by less than 10%.
  - Due to dissipational baryonic processes, DM sphericity systematically higher in the hydrodynamic simulations compared to DMO haloes in which $s = [0.75, 0.85]$.

Halo shapes

- Describe a deviation from sphericity by the triaxiality parameter:

$$T = \frac{a^2 - b^2}{a^2 - c^2}$$

- Oblate systems, $a \approx b \gg c \Rightarrow T \approx 0$.

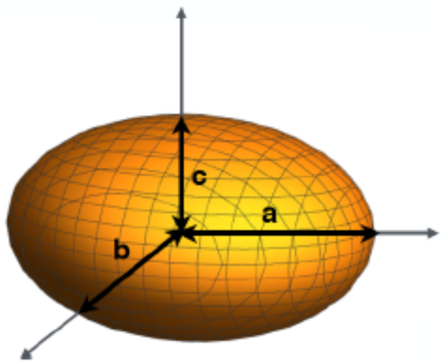

- Prolate systems, $a \gg b \approx c \Rightarrow T \approx 1$.

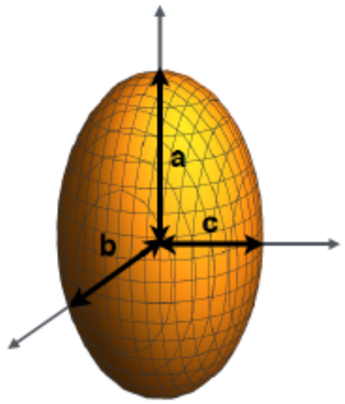

- In the hydro case, since inner haloes are very close to spherical, deviation towards either oblate or prolate is small. DMO counterparts have a preference for *prolate* inner haloes.

Parameters of the simulations

Simulation	code	$N_{\rm DM}$	$m_{\rm g}$ [$M_\odot$]	$m_{\rm DM}$ [$M_\odot$]	ϵ [pc]
Ling *et al.*	RAMSES	2662	–	7.46×10^5	200
Eris	GASOLINE	81213	2×10^4	9.80×10^4	124
NIHAO	EFS-GASOLINE2	–	3.16×10^5	1.74×10^6	931
EAGLE (HR)	P-GADGET (ANARCHY)	1821–3201	2.26×10^5	1.21×10^6	350
APOSTLE (IR)	P-GADGET (ANARCHY)	2160, 3024	1.3×10^5	5.9×10^5	308
MaGICC	GASOLINE	4849, 6541	2.2×10^5	1.11×10^6	310
Sloane *et al.*	GASLOINE	5847–7460	2.7×10^4	1.5×10^5	174

Properties of the selected MW analogues

Simulation	Count	$M_{\rm star}$ [$\times 10^{10} M_\odot$]	$M_{\rm halo}$ [$\times 10^{12} M_\odot$]	ρ_χ [GeV/cm^3]	$v_{\rm peak}$ [km/s]
Ling *et al.*	1	~ 8	0.63	0.37–0.39	239
Eris	1	3.9	0.78	0.42	239
NIHAO	5	15.9	~ 1	0.42	192–363
EAGLE (HR)	12	4.65–7.12	2.76–14.26	0.42–0.73	232–289
APOSTLE (IR)	2	4.48, 4.88	1.64–2.15	0.41–0.54	223–234
MaGICC	2	2.4–8.3	0.584, 1.5	0.346, 0.493	187, 273
Sloane *et al.*	4	2.24–4.56	0.68–0.91	0.3–0.4	185–204